PACIFIC COLLECTION
RECEIVED 15/01/07

THE UNIVERSITY OF THE SOUTH PACIFIC
LIBRARY

DIGITAL THESES PROJECT

Author Statement of Accessibility- Part 2- Permission for Internet Access

Name of Candidate : ASHEHAD ASHWEEN ALI

Degree : MSc - APPLIED MATHEMATICS

Department/School : The University of the South Pacific

Institution/University : SCHOOL OF CIMS, USP, SUVA.

Thesis Title : A SOLUTION TO FINDPATH PROBLEM OF ANCHORED & UNANCHORED MANIPULATORS IN CONSTRAINED ENVIRONMENTS.

Date of completion of requirements for award : 23/11/06

1. I authorise the University to make this thesis available on the Internet for access by USP authorised users. [✓ Yes]/No

2. I authorise the University to make this thesis available on the Internet under the International digital theses project [✓ Yes]/No

Signed:

Date: 27/11/06

Contact Address	**Permanent Address**
SCHOOL OF CIMS	LOT 247, FLETCHER RD,
USP, SUVA	VATUWAQA,
Ph: 3232598	SUVA
e-mail : ali_a@usp.ac.fj	e-mail: ali_a@usp.ac.fj

A Solution to the Findpath Problem of Anchored and Unanchored Manipulators in Constrained Environments

Declaration of Originality

I declare that this thesis which I have presented for consideration for my master's degree embodies the results of my own study and research and has been composed by myself unless otherwise stated.

Ashehad Ashween Ali

January, 2006.

A Solution to the Findpath Problem of Anchored and Unanchored Manipulators in Constrained Environments

by

Ashehad Ashween Ali [1]

Submitted to the

Faculty of Science and Technology in partial fulfilment of the
requirements for the degree of

Master of Science in Applied Mathematics

at the

University of the South Pacific

January, 2006.

---

[1] ali_a@usp.ac.fj

A Solution to the Findpath Problem of Anchored and Unanchored Manipulators in Constrained Environments

by

Ashehad Ashween Ali

Submitted to the Faculty of Science and Technology

in partial fulfilment of the requirements for the

degree of Master of Science in Applied Mathematics

Abstract

This research intends to explore the fundamentals of an emerging technique, applicable at least, in principle, to motion planning and control of anchored and unanchored manipulators. Termed the the Direct method of Lyapunov, currently a powerful mathematical technique used to study the qualitative behaviour of natural or man-made systems that could be modelled, in an approximate way, by differential equations. This research proposes a set of continuous control laws to control the motion of a 3-link planar, anchored manipulators and unanchored (differential drive and car-like) manipulators from an initial configuration to a desired one in constrained environments whilst satisfying holonomic and the nonholonomic constraints of the different systems. These nonlinear controllers are mathematical entities which have been synthesised via a new Lyapunov function, which guarantees stability of the system. Computer simulations are used to illustrate the effectiveness of our new control laws.

Acknowledgements

First and foremost, I would like to thank my advisor Dr Jito Vanualailai. His view of nonlinear dynamical systems and his mathematical discipline taught me to see nonlinear dynamical systems from a perspective that enhanced my understanding of what constitutes an acceptable solution for certain fundamental problems in control theory. I have always valued his advice greatly.

I wish to give my very special thanks to my co-advisor Mr Bibhya Nand Sharma who has been a constant source of support and encouragement for me from the beginning of my research at the University of the South Pacific. His useful comments and invaluable advice on many important occasions were remarkable.

I owe my sincere gratitude to the University of the South Pacific for providing financial support towards my research.

Thank you too, Mr Rinel Ram and Mr Navneet Maharaj for providing useful software. Your help will be remembered forever.

I am incredibly grateful to my family. Their unreserved support and unconditional love were the driving force of my effort.

Contents

List of Figures

List of Tables

Preface

Lyapunov [9] formed a basis of what is now as essential method in the analysis of the behaviour of nonlinear dynamical systems. The Second or the Direct method of Lyapunov is very useful in analysing nonlinear systems as it is able to provide vital information concerning the stability of an equilibrium state of a dynamical system. This single characteristic of the method makes it a useful tool for analysing realistic models which are usually nonlinear, involve large amplitudes and contain several equilibria. To find exact solutions to such models is sometimes beyond our mathematical ability, and hence we are forced to look for an appropriate solution, linearized or to use a computer.

In this thesis, our goal is to solve findpath problems of the anchored and unanchored manipulators and hence establish the stability of the system via Lyapunov method.

In Chapter 1, we present a review of the work that was earlier done, give Lyapunov stability definitions and its theorems and indicate the motivation for motion planning.

In Chapters 2 and 3, we provide detailed derivations of kinematic equations of motion of the 3-link anchored manipulator using geometry in static and dynamic environments respectively. We will consider different scenarios in these chapters and provide controllers for the motion of the manipulators.

Chapter 4 presents derivation of kinematic equations of the motion of a planar dual-arm cooperative manipulators using geometry. Nonlinear controllers that guide the manipulator to its designated target are stated.

In Chapters 5 and 6, we extract nonlinear controllers for differential drive mobile manipulator and car-like drive mobile manipulator, respectively. The motion planning algorithm developed constructs trajectory inputs that drive both the manipulator and its platform to a final configuration without violating the nonholonomic constraints for both of the mobile manipulator systems.

Chapter 7 provides the conclusion to the thesis. It also gives a brief overview of related research that could be done in future.

Chapter 1

Introduction

1.1 Literature Survey

One of the very interesting problems today is attaining specific configurations in constrained environments. Studies, such as Ha et al. [4], Kantabutra [6], Kreveld et al. [7], Meyer [10] and Vanualailai and Sharma [15], have all looked into the motion problem in constrained environments with the robot arms anchored. These studies have used planar manipulators (with revolute joints) in constrained environments (rectangular, triangular) and searched for final configurations, specific configurations (folding of rulers, Rim Normal configuration) and reachability of points. Vanualailai and Sharma [15] introduced the Lyapunov Method to the findpath problem in constrained environment. They looked at feasible trajectories within a rectangle. The controllers obtained successfully avoided the singularities and moving/fixed obstacles within the path of the links and the final end-effector.

The first part of this thesis on anchored manipulators builds on the concept and ventures into more complicated trajectories with increased number of links in constrained environment. A rectangle would act as constrained environment in this research for the anchored 3-link planar (RR) robot arm and specific tasks would then be carried out.

In the second part, the thesis will concentrate on a 2-link manipulator attached to mobile platforms. Mobile robots consisting of a mobile platform with one or many manipulators, are of great interest for a number of real-life applications. Applications for such systems abound in mining, forestry, planetary exploration and the military. In recent years, there has been a growing interest in path planning and motion control of both holonomic and nonholonomic mobile robots. Barraquand and Latombe [1] derived the nonholonomic constraints for unanchored manipulators and discussed the optimal maneuvering of mobile robots. Carriker, Khosla, and Krogh [2] formulated the coordination of mobility and manipulation as a nonlinear optimization problem. Hootsmans and Dubowsky [5] developed an extended Jacobian transpose control method to compensate for dynamic interactions between the manipulator and the base. Liu and Lewis [8] developed a decentralized robust controller for trajectory tracking of the mobile manipulator's End-effector. Miksch and Schroeder [11] used optimization of a performance functional to derive a controller for a mobile manipulator. Murray and Sastry [12] investigated motion control of nonholonomic systems using sinusoids. Papadopoulos and Poulakakis [4] used Lagrange's method to planning trajectory and control for mobile manipulators. Seraji [14] described a simple on-line method for motion control of mobile manipulators. Yamamoto [16] investigated modeling, control and co-ordination of mobile manipulators.

In the second part of this thesis, we will find feasible trajectories of the differential drive mobile manipulator and car-like mobile manipulator. Motion of these manipulators and platform would be governed by laws extracted from Lyapunov functions.

1.2 Holonomy

A holonomic system is one in which the number of degrees of freedom are equal to the number of coordinates needed to specify the configuration of the system. In the field of mobile robots, the term holonomioc mobile robot is applied to the abstraction called the robot, or base, without regard to the rigid bodies which make up the actual mechanism. Thus, any mobile robot with three degrees of freedom of motion in the plane has become known as a holonomic mobile robot. Holonomic mobile robots are desirable because they do not have kinematics motion constraints, which make path planning and control much simpler. In a holonomic system, return to the original internal (joint) configuration means return to the original system position. Mobile robots with arbitrary planar velocities or ones with only translations are holonomic. Holonomic constraints are the constraints on the position (configuration) of a system of particles. They are completely integrable.

1.3 Nonholonomy

Nonholonomic systems, that were once cause for alarm because of their counterintuitive properties, are now being incorporated into practical systems. Ideas from differential geometry, algebra, and other areas of mathematics have played an important role in this process. Now we are seeing some of these ideas being applied to new problems in motion control, mechanical design, electronics, and indeed in many other areas. Let us consider the following example of a nonholonomic constraint.

$$\dot{x}_G \sin\theta_0 - \dot{y}_G \cos\theta_0 = 0.$$

This constraint is nonholonomic because it cannot be integrated analytically to result in a constraint between the configuration variables of the platform, namely x_G, y_G and θ_0. Such constraints are generally caused by one or several rolling contacts between rigid bodies, and reflect the fact that the wheeled platform must move in the direction of its main axis of symmetry. A differential driven platform with manipulator attached is a typical nonholonomic mechanical system. It can attain any position in the plane of motion with any orientation; hence, the configuration space is three dimensional. However, the velocity of the motion must always satisfy a nonholonomic constraint; thus, the space of achievable velocities is two dimensional.

In a nonholonomic system, return to the original internal (wheel) configuration does not guarantee a return to the original system position. More generally, the system outcome for a nonholonomic system is path-dependent. Because nonholonomy is associated with the mobile platform, while the manipulator is holonomic, the system is then studied as two connected subsystems, the holonomic manipulator and its nonholonomic platform.

This allows one to find an admissible path for the mobile platform that can drive it from an initial position and orientation to a final desirable one.

The differences between manipulator arms and wheeled velocities mostly arise from the existence of two types of kinematic linkages. In a general manner, these linkages (or constraints) are exclusively holonomic, i.e. completely integrable, in the case of manipulator arms, while the wheel-to-ground contact linkage which is common to all wheeled mobile robots is nonholonomic, i.e. not completely integrable. For this reason, it is often said that manipulators are holonomic mechanical systems, and that wheeled mobile robots are nonholonomic. The mobile platform that we have proposed for the links is a car-like vehicle. This car like-vehicle is a nonholonomic system. The reason being is that the wheels do not slip sideways.

1.4 Definitions of Stability

Let us consider a nonlinear differential system of the form

$$\frac{d\mathbf{x}}{dt} = \mathbf{g}(\mathbf{x}), \quad \mathbf{x}(t_0) = \mathbf{x}_0\,, \quad t_0 \geq 0\,, \tag{1.1}$$

where $\mathbf{g} : \mathbb{D} \to \mathbf{R}^n$ is a locally Lipschitz map from a domain $\mathbb{D} \subset \mathbf{R}^n$ into $\mathbf{R}^n$ and $\mathbf{x}(t) = (x_1(t), x_2(t), ..., x_n(t))^T$ with $t \geq t_0 \geq 0$. The system (1.1) is said to be *autonomous* or *time invariant* since $\mathbf{g}$ does not depend explicitly on t. It is assumed that in (1.1), the function $\mathbf{g} = (g_1, g_2, ..., g_n)^T$ is at least continuous with $\mathbf{g} \in C[\mathbf{R}^n, \mathbf{R}^n]$ and is smooth enough to guarantee existence, uniqueness and continuous dependence on the solution $\mathbf{x}(t) = \mathbf{x}(t; \mathbf{x}_0)$. Given below are the list of definitions which will be considered in this thesis.

Definition 1.4.1. (Equilibrium Point) *Any point* $\mathbf{x} \in \mathbb{D}$ *is said to be an equilibrium point of system (1.1) if* $\mathbf{g}(\mathbf{x}) = 0$.

Definition 1.4.2. (Stability) *The equilibrium point* $\mathbf{x} = \mathbf{0}$ *of system (1.1) is called stable if, for each* $\epsilon > 0$, *there is* $\delta = \delta(\epsilon) > 0$ *such that* $\|\mathbf{x}(0)\| < \delta \Rightarrow \|\mathbf{x}(t)\| < \epsilon$, *for all* $t \geq 0$.

Definition 1.4.3. (Asymptotic Stability) *The equilibrium point* $\mathbf{x} = \mathbf{0}$ *of system (1.1) is asymptotically stable if it is stable and* δ *can be chosen such that* $\|\mathbf{x}(0)\| < \delta \Rightarrow \lim_{t\to\infty} \mathbf{x}(t) = \mathbf{0}$.

Definition 1.4.4. (Global Asymptotic Stability) *The equilibrium point* $\mathbf{x} = \mathbf{0}$ *of system (1.1) is globally asymptotically stable if it is asymptotically stable and* $\lim_{t\to\infty} \mathbf{x}(t) = \mathbf{0}$ *for all* $\mathbf{x}_0 \in \mathbf{R}^n$.

Definition 1.4.5. (Region of Attraction or Region of Asymptotic Stability) *Let the origin* $\mathbf{x} = \mathbf{0}$ *be an asymptotically stable point for the system (1.1) where* $\mathbb{D}$ *is the domain containing the origin. Let* $\phi(t; \mathbf{x})$ *be the solution of system (1.1) that starts at initial state* $\mathbf{x}$ *at time* $t = 0$. *The origin of attraction of the origin, denoted by* R_A, *is defined by* $R_A = \{\mathbf{x} \in \mathbb{D} | \phi(t; \mathbf{x}) \to \mathbf{0}$ *as* $t \to \infty\}$.

Definition 1.4.6. (Radially Unbounded) *A scaler function* $V(\mathbf{x})$ *is said to be radially unbounded if* $V(\mathbf{x}) \to \infty$ *as* $\|\mathbf{x}\| \to \infty$.

Stability theory plays a central role in systems theory and engineering. There are different kinds of stability problems that arise in the study of dynamical systems. We will consider the stability of equilibrium points. Stability of equilibrium points is usually characterised in the sense of Lyapunov, who laid the foundation of the theory which now carries his name. An equilibrium point is stable if all solutions starting nearby points stay nearby; otherwise it is unstable. It is asymptotically unstable if all solutions starting at nearby points not only stay nearby but also tend to equilibrium point as time approaches infinity. In the following section, we define the Lyapunov function and give Lyapunov's stability theorems.

1.5 Lyapunov Functions and Stability Theorem

Lyapunov functions can be thought of as modified energy functions. They are used to prove that an equilibrium point is Lyapunov stable and (with extra conditions), an equilibrium point is asumptotically stable. Lyapunov functions and its theory can also be used to estimate the region of attraction. The theory of Lyapunov functions is elegant and simple but proving that a Lyapunov function exists or explicitly finding one for a given problem is another question.

The following definition and the theorem, are cited from Deo [3].

Definition 1.5.1. *Suppose that the origin, $\mathbf{x} = \mathbf{e}$, is an equilibrium state for system (1.1). Let $\mathbb{D}$ be an open neighborhood of $\mathbf{e}$ and $V : \mathbb{D} \to \mathbf{R}$ be a continuously differentiable function. Then we define the derivative of V along the trajectories by differentiating V with respect to time using the chain rule, so*

$$\dot{V}(\mathbf{x}) = \frac{dV(\mathbf{x})}{dt} = \dot{\mathbf{x}} \cdot \nabla V(\mathbf{x}) = \mathbf{g}(\mathbf{x}) \cdot \nabla V(\mathbf{x}) = \sum \mathbf{g}(\mathbf{x}) \frac{\partial V(\mathbf{x})}{\partial x_i},$$

where the subscripts denote the components of $\mathbf{g}$ and $\mathbf{x}$. Then V is a Lyapunov function on $\mathbb{D}$ iff

- **(i)** *V is continuously differentiable on $\mathbb{D}$;*

(ii) $V(\mathbf{e}) = 0$ *and* $V(\mathbf{x}) > 0$ *for all* $\mathbf{x} \in \mathbb{D} \setminus \{\mathbf{e}\}$*;*

(iii) $\left.\frac{dV(\mathbf{x})}{dt}\right|_{(1.1)} \leq 0$ *for all* $\mathbf{x} \in \mathbb{D}$*.*

Theorem 1.5.1. (Lyapunov's Stability Theorem) *Let* $\mathbf{x} = \mathbf{e}$ *be an equilibrium point for the system (1.1) and* $\mathbb{D} \subset \mathbf{R}^n$ *be a domain containing* $\mathbf{x} = \mathbf{e}$*. Let* $\mathbf{V}(\mathbf{x})$ *be a Lyapunov function on an open neighborhood of* $\mathbb{D}$*, then* $\mathbf{x} = \mathbf{e}$ *is stable.*

The scaler function V in the above theorem is called a *Lyapunov function* for system (1.1) on $\mathbb{D}$. To understand therefore the behaviour of trajectories in the neighbourhood of the equilibrium hinges only on discovering a Lyapunov function without the need to find the explicit solutions, which, particularly for nonlinear systems, are usually difficult to formulate in closed form. This single aspect of the Direct method of Lyapunov makes it a powerful tool in the stability analysis of nonlinear systems. The Direct method of Lyapunov is now a critical component in specializations such as control engineering, power system engineering, robotics, neural networks, chaos and economics, to name just a few.

For our applications, where we desire the convergence of trajectories to equilibrium points, Theorem 1.5.1 tells us that stability ensures only boundedness of solutions in a neighbourhood of $\mathbf{e}$. However, it is known that if in addition $\mathbf{g}(\mathbf{x})$ is bounded for $\mathbf{x}$ bounded, whenever, $d[V(\mathbf{x})]/dt < 0$ for $\mathbf{x} = \mathbf{e}$ and $d[V(\mathbf{x})]/dt = 0$ in Theorem 1.5.1, the equilibrium point $\mathbf{e}$ is not only stable, but also attracts trajectories to it. That is, $\mathbf{e}$ is *asymptotically stable*, which is clearly more desirable than stability from a practical point of view. In this thesis, to simplify our discussion, it is suffice to guarantee stability. The computer is then used to find initial conditions that guarantee attraction.

1.6 Motivation

The reason that there is so much research in motion planning is based greatly on technological advances of our time. Today, robots have started taking the place of doctors in several fields of medical surgery namely the ones that require perfect precision such as brain surgeries. Thus, there is a need to do motion planning of dynamical systems, which is also termed as the Findpath problem. Findpath problem can also be applied to model the motions of molecules, the population dynamics of Human-Exploited Fish/mahogany populations, plant and animal breeding, etc. Furthermore, it is also applicable to control of vehicles, aircraft and spacecraft navigation.

Chapter 2

Anchored Manipulator in Static Environment

2.1 Introduction

This chapter looks into the detailed derivation of kinematic equations of motion for the 3-link anchored manipulator using geometry. In Scenario 1, we use these equations and apply Lyapunov's second method to formulate the controllers that guide the End-effector to its designated target in the rectangle without having collision with the fixed obstacle.

In Scenario 2, we subject the 3-link anchored manipulator to a vertical constraint surface and state its first-order differential equations. Next, a Lyapunov function is constructed which takes into account these functions and the controllers that control the motion are extracted. The animation of the manipulator and the behaviour of the controllers are illustrated under the computer simulation.

2.2 Scenario 1: System Description

Consider the simplified robot arm in a rectangle shown below in Figure 2.1.

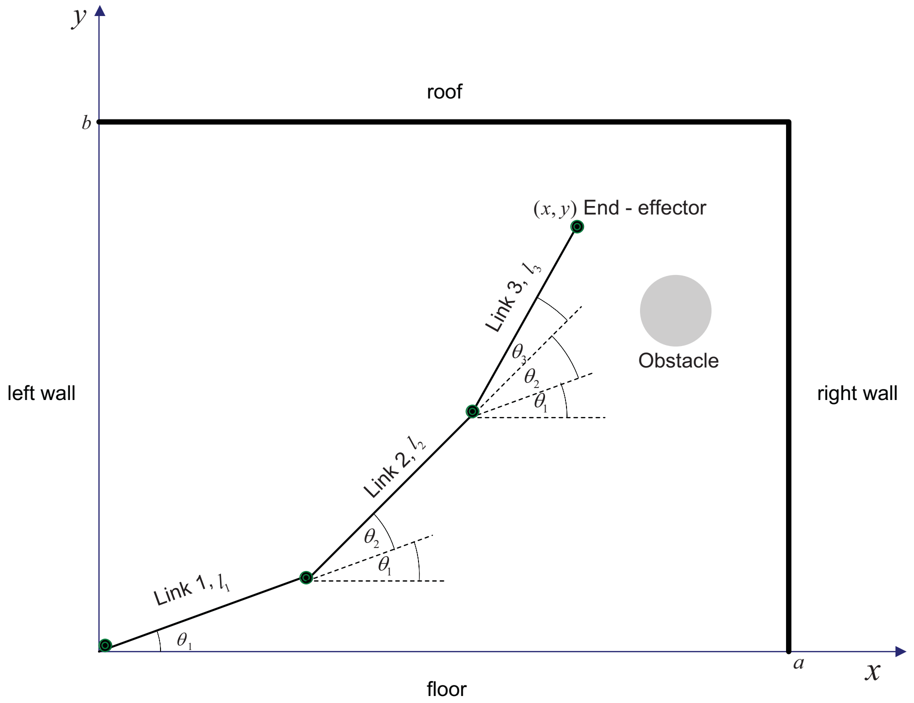

Figure 2.1: A schematic representation of the simplified robot arm in a rectangle.

The position $(x(t), y(t))$ of the End-effector at time t is given by the forward kinematic equations

$$\left.\begin{aligned} x(t) &= l_1 \cos\theta_1(t) + l_2 \cos(\theta_1(t) + \theta_2(t)) + l_3 \cos(\theta_1(t) + \theta_2(t) + \theta_3(t))\,, \\ y(t) &= l_1 \sin\theta_1(t) + l_2 \sin(\theta_1(t) + \theta_2(t)) + l_3 \sin(\theta_1(t) + \theta_2(t) + \theta_3(t))\,, \end{aligned}\right\} \tag{2.1}$$

in which l_1, l_2 and l_3 are the lengths of the three links, respectively. In order to follow a contour at constant velocity, or at any prescribed velocity we must know the relationship between the velocity of the End-effector and the joint velocities. Thus, we differentiate equation (2.1) to obtain the instantaneous velocity as

$$\left.\begin{aligned} \dot{x}(t) &= -\dot{\theta}_1(t)y - \dot{\theta}_2(t)(y - l_1 \sin\theta_1(t)) - \dot{\theta}_3(t)(y - l_1 \sin\theta_1(t) - l_2 \sin(\theta_1 + \theta_2))\,, \\ \dot{y}(t) &= \dot{\theta}_1(t)x + \dot{\theta}_2(t)(x - l_1 \cos\theta_1(t)) + \dot{\theta}_3(t)(x - l_1 \cos\theta_1(t) - l_2 \cos(\theta_1 + \theta_2))\,. \end{aligned}\right\} \tag{2.2}$$

We intend to control the End-effector by controlling the angular accelerations, $\ddot{\theta}_1(t)$, $\ddot{\theta}_2(t)$ and $\ddot{\theta}_3(t)$. If we are to achieve this via the second method of Lyapunov, then, we need to have a system of first-order differential equations describing the motion of the planar robot arm. Thus, if we let

$x_1(t) =$ the x-component of the position of the End-effector,

$x_2(t) =$ the y-component of the position of the End-effector,

$x_3(t) =$ the angular position, $\theta_1(t)$, of Link 1,

$x_4(t) =$ the angular position, $\theta_2(t)$, of Link 2,

$x_5(t) =$ the angular position, $\theta_3(t)$, of Link 3,

$x_6(t) =$ the angular velocity, $\dot{\theta}_1(t)$, of Link 1,

$x_7(t) =$ the angular velocity, $\dot{\theta}_2(t)$, of Link 2,

$x_8(t) =$ the angular velocity, $\dot{\theta}_3(t)$, of Link 3,

$u_1(t) =$ the angular acceleration, $\ddot{\theta}_1(t)$, of Link 1,

$u_2(t) =$ the angular acceleration, $\ddot{\theta}_2(t)$, of Link 2,

$u_3(t) =$ the angular acceleration, $\ddot{\theta}_3(t)$, of Link 3,

at time t, then using equation (2.2), we have (on suppressing t),

$$\left.\begin{aligned}
\dot{x}_1 &= -x_6 x_2 - x_7(x_2 - l_1 \sin x_3) - x_8(x_2 - l_1 \sin x_3 - l_2 \sin(x_3 + x_4))\,, \\
\dot{x}_2 &= x_6 x_1 + x_7(x_1 - l_1 \cos x_3) + x_8(x_1 - l_1 \cos x_3 - l_2 \cos(x_3 + x_4))\,, \\
\dot{x}_3 &= x_6\,, \qquad \dot{x}_6 = u_1\,, \\
\dot{x}_4 &= x_7\,, \qquad \dot{x}_7 = u_2\,, \\
\dot{x}_5 &= x_8\,, \qquad \dot{x}_8 = u_3\,.
\end{aligned}\right\} \tag{2.3}$$

We shall use the vector $\mathbf{x} = (x_1, ..., x_8)$ to describe the variables in system (2.3). Also, we define the vector $\mathbf{e} = (p_1, p_2, p_3, p_4, p_5, 0, 0, 0)$ where, (p_1, p_2) is the final configuration of the End-effector at the target and p_3, p_4, p_5 are the angular positions of the arm at the target.

Before we actually start looking for a Lyapunov function for system (2.3), we may want to look for any difficulty inherent in the basic geometric structure of the robot. As shown by Meyer [10], there is indeed a problem: there exists at least one direction in which the End-effector cannot be moved no matter how we choose the joint velocities $\dot{\theta}_1(t)$, $\dot{\theta}_2(t)$ and $\dot{\theta}_3(t)$. This arises when $\theta_2(t) = 0, \pi$ and $\theta_3(t) = 0, \pi$. In our scheme, we may want to avoid these *singular configurations*. We may also want to take into account other constraints of the system. These include, for example, the allowable space or area to work in, or the allowable velocity or acceleration of the End-effector. Hence, we state our *acceleration control scheme* via the Lyapunov method can be stated as follows:

Step 1. Let the final destination of the End-effector be $(x, y) = (p_1, p_2)$, achieved at the angular positions $x_3 = p_3$, $x_4 = p_4$ and $x_5 = p_5$ and let us call $(p_1, p_2, p_3, p_4, p_5, 0, 0, 0)$ the *target*.

Step 2. Identify the system constraints (these include singular configurations) and appropriately construct mathematical functions to model them. Call the constraints *antitargets* or *obstacles* to be avoided .

Step 3. Construct a Lyapunov function such that u_1, u_2 and u_3 render system (4) stable, meaning that $(p_1, p_2, p_3, p_4, p_5, 0, 0, 0)$ is an equilibrium point of system (4) and that the trajectory $(x_1, x_2, x_3, x_4, x_5, x_6, x_7, x_8)$ starts and remains, for all time $t > 0$, near the target $(p_1, p_2, p_3, p_4, p_5, 0, 0, 0)$ while it avoids stationary and/or mobile obstacles in the workspace.

In Step 1, intuitively, we want to have a kind of a yardstick that measures, at time t , the position of the End-effector from the point $(x, y) = (p_1, p_2)$ and the rate at which it approaches or moves away from (p_1, p_2). The following choice of probable functions accomplishes this (on suppressing t),

$$V_0(\mathbf{x}) = \frac{1}{2}\left[(x_1 - p_1)^2 + (x_2 - p_2)^2 + x_6^2 + x_7^2 + x_8^2\right],$$

noting that $V_0(\mathbf{e}) = 0$ and $V_0(\mathbf{x}) > 0$ for $\mathbf{x} \neq \mathbf{e}$. Again referring to Appendix A-7.1, in Step 3, if a trajectory ever converges to the target, then it remains there for all time t since $V_0(\mathbf{e}) = 0$. The use of V_0, together with appropriate collision avoidance schemes, should enable us to construct Lyapunov functions that ensure that trajectories remain near $\mathbf{e}$ while avoiding abstacles.

2.3 Possible Avoidance Functions

2.3.1 Avoidance of Singular Configurations.

The singular configurations occur when $\theta_2 = x_4 = 0, \pi$ and $\theta_3 = x_5 = 0, \pi$ in the anti-clockwise direction or $\theta_2 = x_4 = -\pi$ and $\theta_3 = x_5 = -\pi$ in the clockwise direction. For the configuration, consider the functions

$$W_1(\mathbf{x}) = |x_4| \tag{2.4}$$

$$W_2(\mathbf{x}) = \pi - |x_4| \tag{2.5}$$

$$W_3(\mathbf{x}) = |x_5| \tag{2.6}$$

$$W_4(\mathbf{x}) = \pi - |x_5|, \tag{2.7}$$

for both x_4 and $x_5 \in (-\pi, 0) \cup (0, \pi)$.

Now, let us, for the moment, consider the effect of the ratios

$$\frac{\beta_1}{W_1}, \frac{\beta_2}{W_2}, \frac{\beta_3}{W_3} \text{ and } \frac{\beta_4}{W_4},$$

for some constants $\beta_1, \beta_2, \beta_3$ and β_4. If the robot arm approaches any one of the singular configurations, it is clear that one of the ratios will increase. Hence if the ratios form parts of the Lyapunov function for system (2.3), intuitively the ratios will act as avoidance functions that repel the robot arm from the singular configurations. Indeed, by the mere fact that we will have a Lyapunov function, all trajectories will converge to the neighbourhood of the target, implying therefore that we cannot have the situation where $W_1 = W_2 = W_3 = W_4 = 0$. This in turn means that we cannot have, at any time, the angular position of Link 2 and Link 3 as $p_4 = -\pi, 0, \pi$ and $p_5 = -\pi, 0, \pi$. So, we can think about singular configurations as mobile obstacles.

The motion of the arm is restricted within the rectangle. We place the bottom left corner of the rectangle at $(0, 0)$ where the base of the arm is located, as shown in Figure 2.1 on page 10, in which we call the constraints the *left wall, right wall, floor, roof* and *circular obstacle*. These are fixed obstacles. We will also call the joint between Link 1 and Link 2 to be the First elbow and the joint between Link 2 and Link 3 to be the Second elbow. The mobile obstacles are the singular configurations.

For obvious geometrical reasons, we construct the following avoidance functions in Table 2.1 that ensure that the Eend-effector does not collide with the obstacles.

2.3.2 Avoidance Functions for the End-effector.

Table 2.1 accommodates an array of repulsive potential functions that will ensure that the End-effector, Link 1, the First and the Second elbows, do not collide with the boundaries of the rectangle and the Circle. Note, it only necessitates to create avoidance functions for the links and the elbows if they physically collide with any of the boundaries of the rectangle.

2.4 Obstacle Avoidance and Target Attraction.

The Lyapunov function of our system must be exactly zero at the target center.

Consequently we introduce:

$$F_0(\mathbf{x}) = \frac{1}{2}\left[(x_1 - p_1)^2 + (x_2 - p_2)^2\right] \geq 0 \tag{2.8}$$

Table 2.1: Array of repulsive potential functions

Obstacle	Functions for obstacle avoidance	Sign
End-effector to avoid:		
Left wall, $x_1 = 0$	$W_5 = x_1$	$W_5 > 0, \forall\, x_1 \in (0, a)$
Right wall, $x_1 = a$	$W_6 = a - x_1$	$W_6 > 0, \forall\, x_1 \in (0, a)$
Floor, $x_2 = 0$	$W_7 = x_2$	$W_7 > 0, \forall\, x_2 \in (0, b)$
Roof, $x_2 = b$	$W_8 = b - x_2$	$W_8 > 0,\ \forall x_2 \in (0, b)$
Link 1 to avoid:		
Floor, $x_3 = 0$	$W_9 = x_3$	$W_9 > 0, \forall\, x_3 \in (0, \pi/2)$
Left wall, $x_3 = \pi/2$	$W_{10} = \pi/2 - x_3$	$W_{10} > 0, \forall\, x_3 \in (0, \pi/2)$
First elbow to avoid:		
Roof, $x_2 = b$	$W_{11} = b - l_1 \sin x_3$	$W_{11} > 0$
Right wall, $x_1 = a$	$W_{12} = a - l_1 \cos x_3$	$W_{12} > 0$
Second elbow to avoid:		
Roof, $x_2 = b$	$W_{13} = b - (l_1 \sin x_3 + l_2 \sin(x_3 + x_4))$	$W_{13} > 0$
Right wall, $x_1 = a$	$W_{14} = a - (l_1 \cos x_3 + l_2 \cos(x_3 + x_4))$	$W_{14} > 0$
Floor, $x_2 = 0$	$W_{15} = l_1 \sin x_3 + \lvert l_2 \sin(x_3 + x_4)\rvert$	$W_{15} > 0$
Left wall, $x_1 = 0$	$W_{16} = l_1 \cos x_3 + \lvert l_2 \cos(x_3 + x_4)\rvert$	$W_{16} > 0$
End-effector to avoid:		
Circle	$W_{17} = \frac{1}{2}\{(x_1 - o_1)^2 + (x_2 - o_2)^2 - (ro)^2\}$	$W_{17} > 0$

2.4.1 A Lyapunov Function

Consider the tentative Lyapunov function,

$$V(\mathbf{x}) = V_0(\mathbf{x}) + F_0(\mathbf{x}) \sum_{i=1}^{17} \frac{\beta_i}{W_i(\mathbf{x})}, \tag{2.9}$$

where β_i is a positive constant.

Clearly, V is continuous and positive on the domain

$$\mathbb{D}(V) = \{\mathbf{x} \in \mathbf{R}^8 : W_i > 0, i = 1, ..., 17\}.$$

Along a particular trajectory of system (2.3), we have (on suppressing t),

$$\begin{aligned} \dot{V}(\mathbf{x}) &= \dot{V}_0(\mathbf{x}) + \dot{F}_0(\mathbf{x}) \sum_{i=1}^{17} \frac{\beta_i}{W_i} - F_0(\mathbf{x}) \sum_{i=1}^{17} \frac{\beta_i \dot{W}_i}{W_i^2} \\ &= \{G_1(\mathbf{x}) + u_1\}x_6 + \{G_2(\mathbf{x}) + u_2\}x_7 + \{G_3(\mathbf{x}) + u_3\}x_8 \end{aligned}$$

where $G_1(\mathbf{x}), G_2(\mathbf{x})$ and $G_3(\mathbf{x})$ are clearly defined in Appendix A.1. Also, we see that for $\mathbf{e} = (p_1, p_2, p_3, p_4, p_5, 0, 0, 0)$, we have $V(\mathbf{e}) = \mathbf{0}$, and since $\mathbf{e} \in \mathbb{D}(V)$, we may take $\mathbb{D}(V)$ as the neighbourhood $\mathbb{D}$ of the point $\mathbf{e}$.

Now, for some numbers $\alpha_1 > 0$, $\alpha_2 > 0$ and $\alpha_3 > 0$, define

$-\alpha_1 x_6 = G_1 + u_1$, $-\alpha_2 x_7 = G_2 + u_2$ and $-\alpha_3 x_8 = G_3 + u_3$.

Then

$$\dot{V}(\mathbf{x}) = -\alpha_1 x_6^2 - \alpha_2 x_7^2 - \alpha_3 x_8^2 \leq 0,$$

provided we have $u_1 = -\alpha_1 x_6 - G_1$, $u_2 = -\alpha_2 x_7 - G_2$ and $u_3 = -\alpha_3 x_8 - G_3$ as the *nonlinear controllers*. Since $\dot{V}(\mathbf{x})$ is nonpositive and continuous for all $\mathbf{x} \in \mathbb{D}(V)$, by Lyapunov's stability Theorem 1.5.1, V is a Lyapunov function for system (2.3) on $\mathbb{D}(V)$ establishing the stability of $\mathbf{e}$. Hence, $\mathbf{e}$ is an equilibrium point of system (2.3), and our

Lyapunov function satisfies Theorem 1.5.1 at this equilibrium point.

Thus, we have the system

$$\left.\begin{aligned}
\dot{x}_1 &= -x_6x_2 - x_7(x_2 - l_1\sin x_3) - x_8(x_2 - l_1\sin x_3 - l_2\sin(x_3+x_4))\,, \\
\dot{x}_2 &= x_6x_1 + x_7(x_1 - l_1\cos x_3) + x_8(x_1 - l_1\cos x_3 - l_2\cos(x_3+x_4))\,, \\
\dot{x}_3 &= x_6\,, \qquad \dot{x}_6 = -\alpha_1 x_6 - G_1\,, \\
\dot{x}_4 &= x_7\,, \qquad \dot{x}_7 = -\alpha_2 x_7 - G_2\,, \\
\dot{x}_5 &= x_8\,, \qquad \dot{x}_8 = -\alpha_3 x_8 - G_3\,,
\end{aligned}\right\} \tag{2.10}$$

which is stable at the equilibrium point $\mathbf{e} = (p_1, p_2, p_3, p_4, p_5, 0, 0, 0)$.

2.5 A Computer Simulation

The computer is used to numerically integrate system (2.10) to obtain the solution $(x_1, ..., x_8)$ and plot the points $(x_1(t), x_2(t))$ at time t in the x_1x_2-plane until the points converge to a neighbourhood of (p_1, p_2) and stay there as $t \to \infty$. For our example, Table 2.2 below gives the parameters, and Figure 2.2 on page 21 gives the trajectory of the arm. Notice the slowing down of the arm as it approaches its final configuration. This could be explained in terms of the potential energy "cup" of the Lyapunov function derived by Vanualailai and Bibhya [15]. The arm reaches its final configuration in about 10 units of time. In Figure 2.2 on page 21, the first five links are drawn every 1 unit of time.

Figure 2.3 on page 22 shows the behaviour of the controllers, u_1 (dashed line), u_2 (bold line) and u_3 (solid line) which converge to 0 as time $t \to \infty$.

Table 2.2: A Scenario 1 example

Lengths of Links	$l_1 = 3, l_2 = 2.5$ and $l_3 = 2$
Initial Conditions	$\mathbf{x} = (3, 3, \pi/3, -2\pi/3, 2\pi/3, \pi/180, \pi/180, \pi/180)$
Planar Target	$(p_1, p_2) = (2, 5)$
Control Parameters	$\beta_1 = \beta_2 = \beta_3 = \beta_4 = \beta_{14} = \beta_{16} = 0.01,$ $\beta_{12} = 0.05, \beta_5 = 0.1, \beta_{11} = 0.5,$ $\beta_8 = \beta_9 = \beta_{10} = \beta_{13} = 1,$ $\beta_6 = 10, \beta_{15} = 20, \beta_7 = 30$ and $\beta_{17} = 0.000001$
Convergence Parameters	$\alpha_1 = 80, \alpha_2 = 90$ and $\alpha_3 = 100$
Right wall, Roof	$a = 4.5$ and $b = 6$
Circular Obstacle Center	$o_1 = 2.7$ and $o_2 = 3.5$
Circular Obstacle Radius	$ro = 1$

2.5.1 Remark

Under the proposed controllers, we saw that the anchored manipulator reached its target whilst avoiding colliding with the fixed obstacle and having a safe and smooth trajectory.

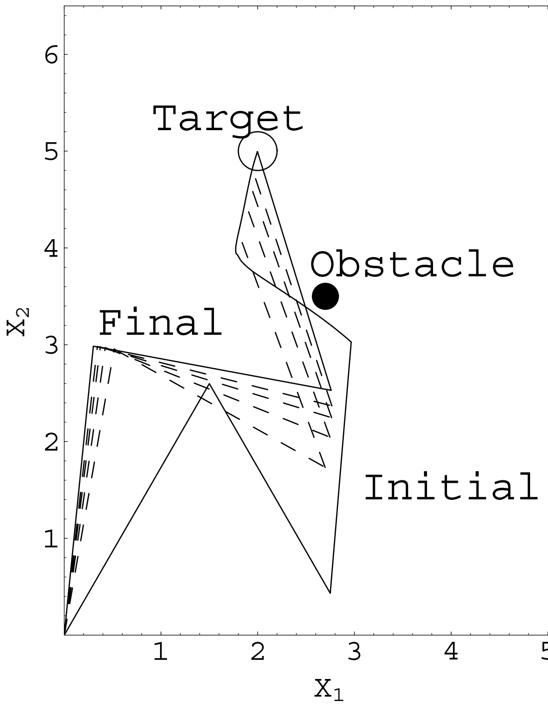

Figure 2.2: Animation of the motion of the anchored manipulator.

2.6 Scenario 2 : System Description

Consider the robot arm in Figure 2.4 on page 23. We force the robot arm to be in contact with the constraint surface (wall) and allow it only to move in vertical direction.

The description of the variables remain the same as it were in Section 2.2. Now we state

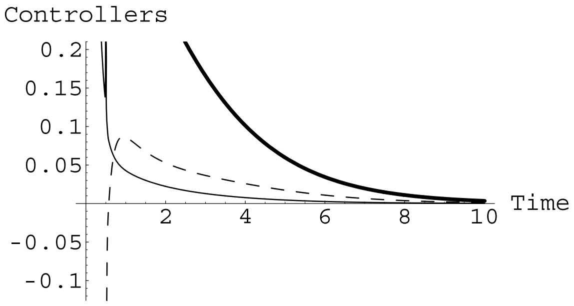

Figure 2.3: Behaviour of the nonlinear controllers; u_1 (dashed line), u_2 (bold line) and u_3 (solid line).

space equations describing the motion of the planar robot arm,

$$\begin{cases} \dot{x}_1 = -x_6 x_2 - x_7(x_2 - l_1 \sin x_3) - x_8(x_2 - l_1 \sin x_3 - l_2 \sin(x_3 + x_4)) \,, \\ \dot{x}_2 = x_6 x_1 + x_7(x_1 - l_1 \cos x_3) + x_8(x_1 - l_1 \cos x_3 - l_2 \cos(x_3 + x_4)) \,, \\ \dot{x}_3 = x_6 \,, \qquad \dot{x}_6 = u_1 \,, \\ \dot{x}_4 = x_7 \,, \qquad \dot{x}_7 = u_2 \,, \\ \dot{x}_5 = x_8 \,, \qquad \dot{x}_8 = u_3 \,. \end{cases} \tag{2.11}$$

We shall use the vector $\mathbf{x} = (x_1, ..., x_8)$ to describe the variables in system (2.11). Also, we define the vector $\mathbf{e} = (p_1, p_2, p_3, p_4, p_5, 0, 0, 0)$ where, (p_1, p_2) is the final configuration of the End-effector at the target and p_3, p_4, p_5 are the angular positions of the arm at the target.

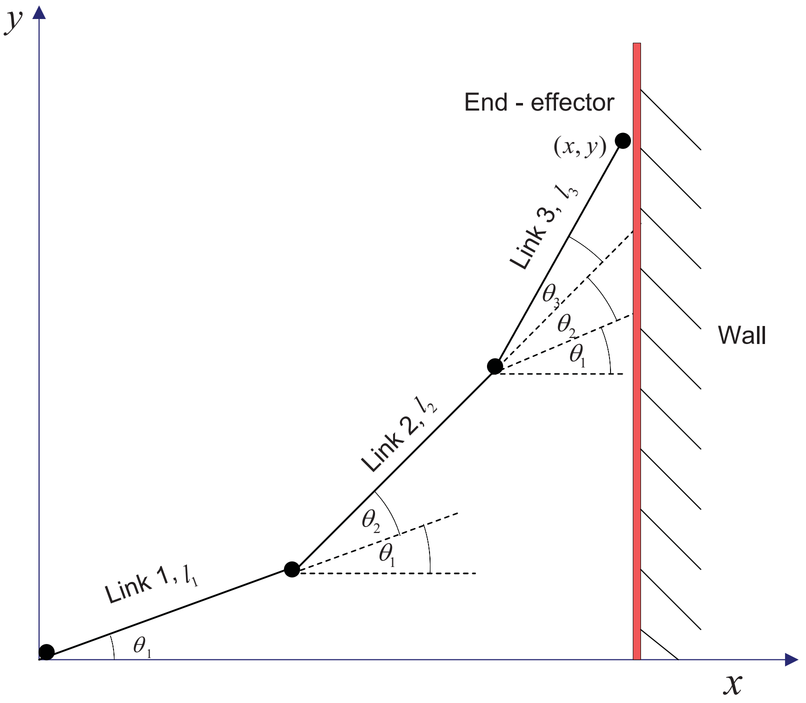

Figure 2.4: A schematic representation of the simplified robot arm in relation to a constraint surface.

2.6.1 A Lyapunov Function

We consider a tentative Lyapunov function and the controllers, the derivation is similar to that in the previous case. For constants $\beta_i > 0$, $i = 1, ..., 5$, we consider

$$V(\mathbf{x}) = V_1(\mathbf{x}) + F_1(\mathbf{x}) \sum_{i=1}^{5} \frac{\beta_i}{W_i(\mathbf{x})},$$

on the domain

$$\mathbb{D}(V) = \{\mathbf{x} \in \mathbf{R}^8 : W_i > 0, i = 1, ..., 5\}$$

where W_1, W_2, W_3, W_4, are equations (2.4), (2.5), (2.6) and (2.7) respectively.

Referring to Figure 2.4 on page 21, we see that the robot arm is to move in the vertical direction only. The x-component of the End-effector is x_1 which thus should not change unlike the y-component of the End-effector. Since the initial value of the x-component of the End-effector will be known, we form a function W_5 as shown below. We choose a_1 in such a way so that a_1 is close to but smaller than the initial value of x_1. The main purpose of W_5 is to restrict the End-effector in a sufficiently small interval between $x = a$ and the right wall. Thus we have

$$W_5(\mathbf{x}) = x_1 - a_1,$$

and define

$$V_1(\mathbf{x}) = |x_2 - p_2| + |x_6| + |x_7| + |x_8|,$$

$$F_1(\mathbf{x}) = |x_2 - p_2| \geq 0.$$

Then along a particular trajectory of system (2.11) in $\mathbb{D}(V)$, we have, for $\alpha_1 > 0$, $\alpha_2 > 0$ and $\alpha_3 > 0$, the time-derivative

$$\dot{V}(\mathbf{x}) = -\alpha_1 x_6^2 - \alpha_2 x_7^2 - \alpha_3 x_8^2,$$

if we define the controllers as $u_1 = (-\alpha_1 x_6 - G_4)|x_6|$, $u_2 = (-\alpha_2 x_7 - G_5)|x_7|$ and $u_3 = (-\alpha_3 x_8 - G_6)|x_8|$, where G_4, G_5 and G_6 are defined in Appendix A.2. Also, we see that for $\mathbf{e} = (p_1, p_2, p_3, p_4, p_5, 0, 0, 0)$, we have $V(\mathbf{e}) = \mathbf{0}$, and since $\mathbf{e} \in \mathbb{D}(V)$, we may take $\mathbb{D}(V)$ as the neighbourhood $\mathbb{D}$ of the point $\mathbf{e}$. Hence, $\mathbf{e}$ is an equilibrium point of system (2.11), and our Lyapunov function satisfies Theorem 1.5.1 at this equilibrium point.

Thus, we have the system

$$\begin{cases} \dot{x}_1 = -x_6x_2 - x_7(x_2 - l_1 \sin x_3) - x_8(x_2 - l_1 \sin x_3 - l_2 \sin(x_3 + x_4)) \,, \\ \dot{x}_2 = x_6x_1 + x_7(x_1 - l_1 \cos x_3) + x_8(x_1 - l_1 \cos x_3 - l_2 \cos(x_3 + x_4)) \,, \\ \dot{x}_3 = x_6 \,, \qquad \dot{x}_6 = -\alpha_1 x_6 - G_4 \,, \\ \dot{x}_4 = x_7 \,, \qquad \dot{x}_7 = -\alpha_2 x_7 - G_5 \,, \\ \dot{x}_5 = x_8 \,, \qquad \dot{x}_8 = -\alpha_3 x_8 - G_6 \,, \end{cases} \tag{2.12}$$

which is stable at the equilibrium point $\mathbf{e} = (p_1, p_2, p_3, p_4, p_5, 0, 0, 0)$.

2.7 A Computer Simulation

The computer is used to numerically integrate system (2.12) to obtain the solution $(x_1, ..., x_8)$ and plot the points $(x_1(t), x_2(t))$ at time t in the x_1x_2-plane until the points converge to a neighbourhood of (p_1, p_2) and stay there as $t \to \infty$. For our example, Table 2.3 below gives the parameters, and Figure 2.5 on page 26 gives the trajectory of the arm. The arm reaches its final configuration in about 20 units of time. In Figure 2.5 on page 26, the first three links are drawn every 1 unit of time.

Table 2.3: A Scenario 2 example

Lengths of Links	$l_1 = 3, l_2 = 2$ and $l_3 = 1$
Initial Conditions	$\mathbf{x} = (4.29788, 2.6157, \pi/3, -\pi/4, -\pi/4, \pi/180, \pi/180, \pi/180)$
Planar Target	$(p_1, p_2) = (4.005135, 3.79907)$
Control Parameters	$\beta_1 = \beta_2 = \beta_3 = \beta_4 = 1$ and $\beta_5 = 0.00005$
Convergence Parameters	$\alpha_1 = 80, \alpha_2 = 80$ and $\alpha_3 = 80$

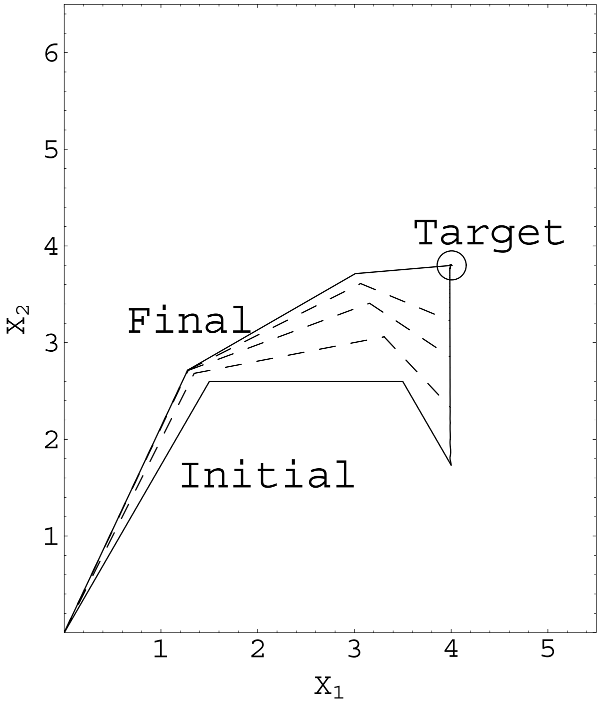

Figure 2.5: Animation of the motion of the anchored manipulator.

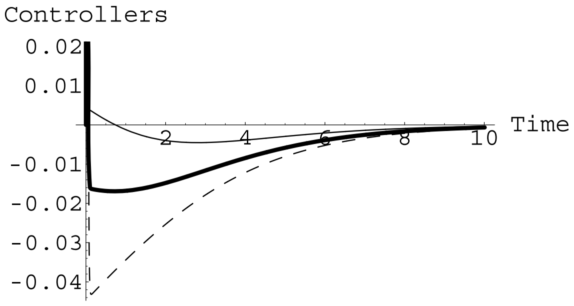

Figure 2.6: Behaviour of the nonlinear controllers; u_1 (dashed line), u_2 (bold line) and u_3 (solid line)

Figure 2.6 above shows the behaviour of the controllers, u_1 (dashed line), u_2 (bold line) and u_3 (solid line) which converge to 0 as time $t \rightarrow \infty$.

2.7.1 Remark

Under the proposed controllers, we saw that the anchored manipulator had a continuous path to its target against the constraint surface. In Figure 2.5 on page 26, it can be noted that the manipulator has a constant linear velocity.

Chapter 3

Anchored Manipulator in a Dynamic Environment

3.1 Introduction

This chapter looks into the detailed derivation of kinematic equations of motion for the 3-link anchored manipulator and a mobile obstacle in a rectangle using geometry. Here, the manipulator is avoiding collision with the mobile obstacle. Then by the use of the equations and applying Lyapunov's second method, we formulate the controllers that guide the manipulator to its designated target in the rectangle without collision with the mobile obstacle.

3.2 Manipulator Avoiding a Mobile Obstacle

We consider the same 3-link anchored manipulator as in Section 2.2. However, in this case the circular obstacle is no longer fixed but indeed mobile in the workspace of the robot.

For the manipulator, let:

$x_1(t)$ = the x-component of the position of the End-effector,

$x_2(t)$ = the y-component of the position of the End-effector,

$x_3(t)$ = the angular position, $\theta_1(t)$, of Link 1,

$x_4(t)$ = the angular position, $\theta_2(t)$, of Link 2,

$x_5(t)$ = the angular position, $\theta_3(t)$, of Link 3,

$x_6(t)$ = the angular velocity, $\dot{\theta}_1(t)$, of Link 1,

$x_7(t)$ = the angular velocity, $\dot{\theta}_2(t)$, of Link 2,

$x_8(t)$ = the angular velocity, $\dot{\theta}_3(t)$, of Link 3,

$u_1(t)$ = the angular acceleration, $\ddot{\theta}_1(t)$, of Link 1,

$u_2(t)$ = the angular acceleration, $\ddot{\theta}_2(t)$, of Link 2,

$u_3(t)$ = the angular acceleration, $\ddot{\theta}_3(t)$, of Link 3,

For the obstacle, let:

$x_9(t)$ = the x-component of the midpoint of the moving circle,

$x_{10}(t)$ = the y-component of the midpoint of the moving circle,

$x_{11}(t)$ = the angular velocity, $\dot{x}_9(t)$, of the moving circle,

$x_{12}(t)$ = the angular velocity, $\dot{x}_{10}(t)$, of the moving circle,

$u_4(t)$ = the angular acceleration, $\dot{x}_{11}(t)$, of the moving circle,

$u_5(t)$ = the angular acceleration, $\dot{x}_{12}(t)$, of the moving circle.

Then, at time t and using equation (2.2), we have (on suppressing t),

$$\left.\begin{aligned}
\dot{x}_1 &= -x_6 x_2 - x_7(x_2 - l_1 \sin x_3) - x_8(x_2 - l_1 \sin x_3 - l_2 \sin(x_3 + x_4))\,, \\
\dot{x}_2 &= x_6 x_1 + x_7(x_1 - l_1 \cos x_3) + x_8(x_1 - l_1 \cos x_3 - l_2 \cos(x_3 + x_4))\,, \\
\dot{x}_3 &= x_6\,, \qquad \dot{x}_6 = u_1\,, \qquad \dot{x}_9 = x_{11}\,, \qquad \dot{x}_{11} = u_4 \\
\dot{x}_4 &= x_7\,, \qquad \dot{x}_7 = u_2\,, \qquad \dot{x}_{10} = x_{12}\,, \qquad \dot{x}_{12} = u_5 \\
\dot{x}_5 &= x_8\,, \qquad \dot{x}_8 = u_3\,.
\end{aligned}\right\} \tag{3.1}$$

We shall use the vector $\mathbf{x} = (x_1, ..., x_{12})$ to describe the variables in system (3.1). Also, we define the vector $\mathbf{e} = (p_1, p_2, p_5, p_6, p_7, 0, 0, 0, p_3, p_4, 0, 0)$ where for the manipulator, (p_1, p_2) is the final configuration of the End-effector to its target and p_5, p_6, p_7 are the angular positions of the arm at the target. For the obstacle, (p_3, p_4) is the final configuration of the obstacle to its target. The occurrence of singular configuration remains the same as in Subsection 2.3.1 on page 15. Other possible avoidance functions also remain the same except the avoidance function due to mobile obstacle.

3.3 Avoidance Function

3.3.1 Avoidance Function for the End-effector.

Table 3.1 gives the function that will ensure that the End-effector does not collide with the moving circular object .

Table 3.1: Avoidance function for the End-effector.

Obstacle	Avoidance Function	Sign
Circle	$W_{17} = \frac{1}{2}\{(x_1 - x_9)^2 + (x_2 - x_{10})^2 - (ro)^2\}$	$W_{17} > 0$

3.4 Obstacle Avoidance and Target Attraction.

The Lyapunov function of our system must be exactly zero at the target center. Consequently we introduce:

$$F_2(\mathbf{x}) = \frac{1}{2}\left[(x_1 - p_1)^2 + (x_2 - p_2)^2 + (x_9 - p_3)^2 + (x_{10} - p_4)^2\right] \geq 0 \tag{3.2}$$

3.4.1 A Lyapunov Function

Consider the tentative Lyapunov function,

$$V(\mathbf{x}) = V_2(\mathbf{x}) + F_2(\mathbf{x}) \sum_{i=1}^{17} \frac{\beta_i}{W_i(\mathbf{x})}, \tag{3.3}$$

where β_i is a positive constant,

$$V_2(\mathbf{x}) = \frac{1}{2}[(x_1 - p_1)^2 + (x_2 - p_2)^2 + (x_9 - p_3)^2 + (x_{10} - p_4)^2 + x_6^2 + x_7^2 + x_8^2 + x_{11}^2 + x_{12}^2] \tag{3.4}$$

and $W_i(\mathbf{x}), i = 1, ..., 16$ are those that have been mentioned in Section 2.3.

Clearly, V is continuous and positive on the domain

$$\mathbb{D}(V) = \{\mathbf{x} \ \in \ \mathbf{R}^8 : W_i > 0, i = 1, ..., 17\}$$

Along a particular trajectory of system (3.1), we have (on suppressing t),

$$\begin{aligned}
\dot{V}(\mathbf{x}) &= \dot{V}_2(\mathbf{x}) + \dot{F}_2(\mathbf{x}) \sum_{i=1}^{17} \frac{\beta_i}{W_i} - F_2(\mathbf{x}) \sum_{i=1}^{17} \frac{\beta_i \dot{W}_i}{W_i^2} \\
&= \{G_1(\mathbf{x}) + u_1\}x_6 + \{G_2(\mathbf{x}) + u_2\}x_7 + \{G_3(\mathbf{x}) + u_3\}x_8 \\
&\quad + \{G_4(\mathbf{x}) + u_4\}x_{11} + \{G_5(\mathbf{x}) + u_5\}x_{12}
\end{aligned}$$

where $G_1(\mathbf{x}), G_2(\mathbf{x}), G_3(\mathbf{x}), G_4(\mathbf{x})$ and $G_5(\mathbf{x})$ are clearly defined in Appendix A.3. Also, we see that for $\mathbf{e} = (p_1, p_2, p_5, p_6, p_7, 0, 0, 0, p_3, p_4, 0, 0)$, we have $V(\mathbf{e}) = \mathbf{0}$, and since $\mathbf{e} \in \mathbb{D}(V)$, we may take $\mathbb{D}(V)$ as the neighbourhood $\mathbb{D}$ of the point $\mathbf{e}$.

Now, for some numbers $\alpha_1 > 0$, $\alpha_2 > 0$, $\alpha_3 > 0$, $\alpha_4 > 0$ and $\alpha_5 > 0$, define $-\alpha_1 x_6 = G_1 + u_1$, $-\alpha_2 x_7 = G_2 + u_2$, $-\alpha_3 x_8 = G_3 + u_3$, $-\alpha_4 x_{11} = G_4 + u_4$ and $-\alpha_5 x_{12} = G_5 + u_5$.

Then

$$\dot{V}(\mathbf{x}) = -\alpha_1 x_6^2 - \alpha_2 x_7^2 - \alpha_3 x_8^2 - \alpha_4 x_{11}^2 - \alpha_5 x_{12}^2 \leq 0,$$

provided we have $u_1 = -\alpha_1 x_6 - G_1$, $u_2 = -\alpha_2 x_7 - G_2$ $u_3 = -\alpha_3 x_8 - G_3$, $u_4 = -\alpha_4 x_{11} - G_4$ and $u_5 = -\alpha_5 x_{12} - G_5$ as the *nonlinear controllers*. Since $\dot{V}(\mathbf{x})$ is nonpositive and continuous for all $\mathbf{x} \in \mathbb{D}(V)$, by Lyapunov's stability Theorem 1.5.1, V is a Lyapunov function for system (3.1) on $\mathbb{D}(V)$ establishing the stability of $\mathbf{e}$. Hence, $\mathbf{e}$ is an equilibrium point of system (3.1), and our Lyapunov function satisfies Theorem 1.5.1 at this equilibrium point.

Thus, we have the system

$$\left.\begin{array}{ll}
\dot{x}_1 & = -x_6 x_2 - x_7(x_2 - l_1 \sin x_3) - x_8(x_2 - l_1 \sin x_3 - l_2 \sin(x_3 + x_4)) \,, \\
\dot{x}_2 & = x_6 x_1 + x_7(x_1 - l_1 \cos x_3) + x_8(x_1 - l_1 \cos x_3 - l_2 \cos(x_3 + x_4)) \,, \\
\dot{x}_3 & = x_6 \,, \quad \dot{x}_6 = -\alpha_1 x_6 - G_1 \,, \quad \dot{x}_9 = x_{11} \,, \quad \dot{x}_{11} = -\alpha_4 x_{11} - G_4 \,, \\
\dot{x}_4 & = x_7 \,, \quad \dot{x}_7 = -\alpha_2 x_7 - G_2 \,, \quad \dot{x}_{10} = x_{12} \,, \quad \dot{x}_{12} = -\alpha_5 x_{12} - G_5 \,, \\
\dot{x}_5 & = x_8 \,, \quad \dot{x}_8 = -\alpha_3 x_8 - G_3 \,,
\end{array}\right\} \tag{3.5}$$

which is stable at the equilibrium point $\mathbf{e} = (p_1, p_2, p_5, p_6, p_7, 0, 0, 0, p_3, p_4, 0, 0)$.

3.5 A Computer Simulation

The computer is used to numerically integrate system (3.5) to obtain the solution $(x_1, ..., x_{12})$ and plot the points $(x_1(t), x_2(t))$ at time t in the $x_1 x_2$-plane until the points converge to a neighbourhood of (p_1, p_2) and stay there as $t \to \infty$. For our example, Table 3.2 below gives the parameters, and Figure 3.1 on page 34 gives the trajectory of the arm. Notice the slowing down of the arm as it approaches its final configuration. This could be explained in terms of the potential energy "cup" of the Lyapunov function derived by Vanualailai and Bibhya [15]. The arm reaches its final configuration in about 20 units of time. In Figure 3.1 on page 34, the first five links are drawn every 0.25 units of time.

Table 3.2: A Scenario 1 example.

Lengths of Links	$l_1 = 3, l_2 = 2.5$ and $l_3 = 2$
Initial Conditions	$\mathbf{x} = (3, 3, \pi/3, -2\pi/3, 2\pi/3, \pi/180, \pi/180, \pi/180, 1.2, 5, 2, 2)$
Planar Target	$(p_1, p_2) = (2.5, 5)$
Control Parameters	$\beta_1 = \beta_2 = \beta_3 = \beta_4 = \beta_{14} = \beta_{16} = 0.01,$ $\beta_{12} = 0.05, \beta_5 = 0.1, \beta_{11} = 0.5,$ $\beta_8 = \beta_9 = \beta_{10} = \beta_{13} = 1,$ $\beta_6 = 10, \beta_{15} = 2, \beta_7 = 10$ and $\beta_{17} = 0.00001$
Convergence Parameters	$\alpha_1 = 100, \alpha_2 = 200, \alpha_3 = 300, \alpha_4 = 30$ and $\alpha_5 = 300$
Right wall, Roof	$a = 4.5$ and $b = 6$
Circular Obstacle final position	$p_3 = 2$ and $p_4 = 4.3$
Circular Obstacle Radius	$ro = 1$

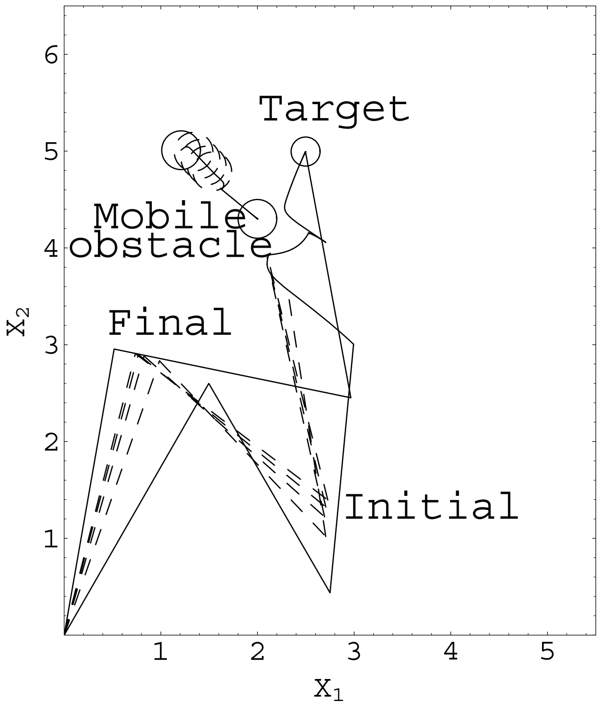

Figure 3.1: Animation of the motion of the anchored manipulator and the mobile obstacle.

In Figure 3.2 on page 35, the controllers are u_1 (dashed line), u_2 (bold line) and u_3 (solid line). In Figure 3.3 on page 35, the controllers are u_4 (dashed line) and u_5 (bold line). These controllers converge to 0 as time $t \to \infty$.

3.5.1 Remark

Under the proposed controllers, we saw that the anchored manipulator avoided collision with the mobile obstacle and reached its target safely while the mobile obstacle also had a smooth trajectory.

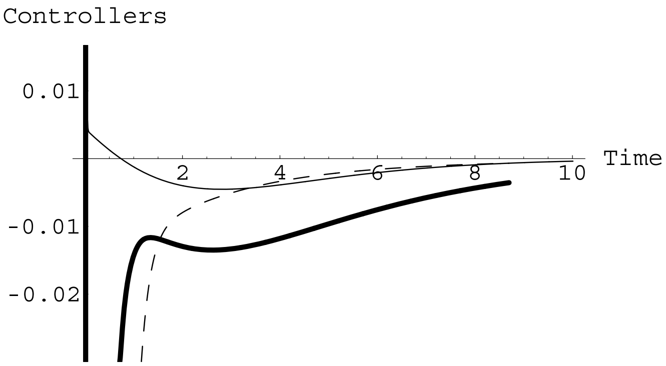

Figure 3.2: Behaviour of the nonlinear controllers; u_1 (dashed line), u_2 (bold line) and u_3 (solid line).

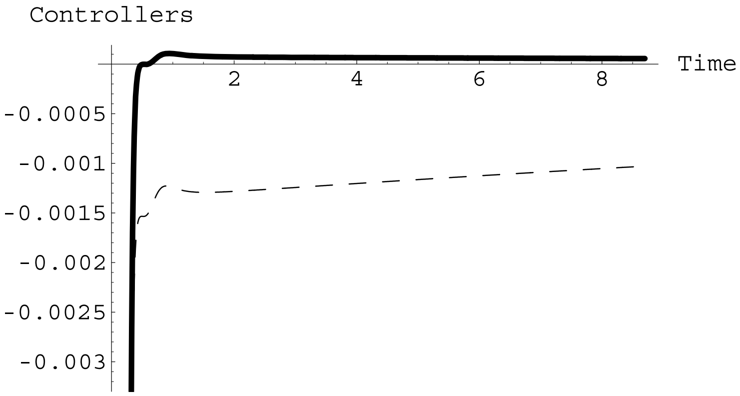

Figure 3.3: Behaviour of the nonlinear controllers; u_4 (dashed line) and u_5 (bold line).

Chapter 4

Dual-Arm Cooperative Manipulators

4.1 Introduction

This chapter looks into the detailed derivation of kinematic equations of motion for a planar dual-arm cooperative manipulators using geometry. Then by the use of these equations and applying Lyapunov's second method, we formulate the controllers that guide the manipulator to its designated target. These anchored manipulators move regular and irregular solids from an initial configuration to a desired one whilst satisfying the holonomic constraints of the system. Computer simulations are used to see the feasibility of achieving collision-free trajectories and pre-defined configurations via our proposed controllers.

4.2 System Description

Before we develop the controller dual-robot-manipulator system, we must first develop a kinematic model for two rigid-link robot manipulators holding a rigid object in a two-dimensional workspace. The overall system is modelled in terms of the kinematics of the two robot manipulators and the rigid object. The configuration of the system is shown in Figure 4.1 on next page. Before we develop the dual-robot-arm model, we state the following assumptions.

Assumption 1.

The kinematics of each manipulator are exactly known.

Assumption 2.

There is no slipping between the manipulator end effectors and the rigid zero degree of freedom object.

Assumption 3.

Each manipulator is a nonredundant rigid robot with serial links connected by six revolute joints.

Figure 4.1 below shows a schematic representation of the dual manipulator system.

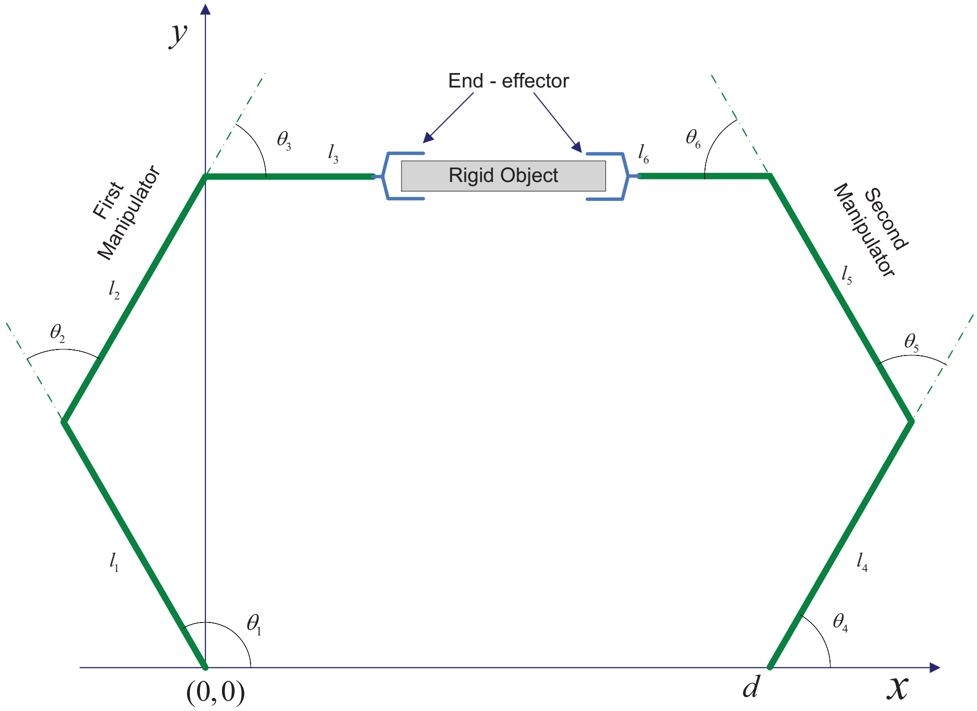

Figure 4.1: Two planar three link robots holding a rigid object.

Referring to Figure 4.1, d is the x-component of the position of the second manipulator. The positions of the End-effectors in the xy-plane for the dual manipulator at time t is given by the forward kinematic equations

$$\left.\begin{aligned} x_1(t) &= l_1\cos\theta_1(t) + l_2\cos(\theta_1(t)+\theta_2(t)) + l_3\cos(\theta_1(t)+\theta_2(t)+\theta_3(t))\,, \\ y_1(t) &= l_1\sin\theta_1(t) + l_2\sin(\theta_1(t)+\theta_2(t)) + l_3\sin(\theta_1(t)+\theta_2(t)+\theta_3(t))\,, \\ x_2(t) &= l_4\cos\theta_4(t) + l_5\cos(\theta_4(t)+\theta_5(t)) + l_6\cos(\theta_4(t)+\theta_5(t)+\theta_6(t)) + d\,, \\ y_2(t) &= l_4\sin\theta_4(t) + l_5\sin(\theta_4(t)+\theta_5(t)) + l_6\sin(\theta_4(t)+\theta_5(t)+\theta_6(t))\,. \end{aligned}\right\} \tag{4.1}$$

The instantaneous velocities are:

$$\left.\begin{aligned}
\dot{x}_1(t) &= -\dot{\theta}_1(t)y_1 - \dot{\theta}_2(t)(y_1 - l_1\sin\theta_1(t)) - \dot{\theta}_3(t)(y_1 - l_1\sin\theta_1(t) - l_2\sin(\theta_1+\theta_2))\,,\\
\dot{y}_1(t) &= \dot{\theta}_1(t)x_1 + \dot{\theta}_2(t)(x_1 - l_1\cos\theta_1(t)) + \dot{\theta}_3(t)(x_1 - l_1\cos\theta_1(t) - l_2\cos(\theta_1+\theta_2))\,,\\
\dot{x}_2(t) &= -\dot{\theta}_4(t)y_2 - \dot{\theta}_5(t)(y_2 - l_4\sin\theta_4(t)) - \dot{\theta}_6(t)(y_2 - l_4\sin\theta_4(t) - l_5\sin(\theta_4+\theta_5))\,,\\
\dot{y}_2(t) &= \dot{\theta}_4(t)x_2 + \dot{\theta}_5(t)(x_2 - l_4\cos\theta_4(t)) + \dot{\theta}_6(t)(x_2 - l_4\cos\theta_4(t) - l_5\cos(\theta_4+\theta_5)).
\end{aligned}\right\} \tag{4.2}$$

4.3 Acceleration Control

We control the End-effector by controlling the angular accelerations, $\ddot{\theta}_1(t)$, $\ddot{\theta}_2(t)$, $\ddot{\theta}_3(t)$, $\ddot{\theta}_4(t)$, $\ddot{\theta}_5(t)$ and $\ddot{\theta}_6(t)$. If we are to achieve this via the second method of Lyapunov, then, we need to have a system of first-order differential equations describing the motion of the planar robot arm.

For the first manipulator, let:

$x_1(t) =$ the x-component of the position of the End-effector,

$x_2(t) =$ the y-component of the position of the End-effector,

$x_5(t) =$ the angular position,$\theta_1(t)$, of Link 1,

$x_6(t) =$ the angular position, $\theta_2(t)$, of Link 2,

$x_7(t) =$ the angular position, $\theta_3(t)$, of Link 3,

$x_{11}(t) =$ the angular velocity, $\dot{\theta}_1(t)$, of Link 1,

$x_{12}(t) =$ the angular velocity, $\dot{\theta}_2(t)$, of Link 2,

$x_{13}(t) =$ the angular velocity, $\dot{\theta}_3(t)$, of Link 3,

$u_1(t) =$ the angular acceleration, $\ddot{\theta}_1(t)$, of Link 1,

$u_2(t) =$ the angular acceleration, $\ddot{\theta}_2(t)$, of Link 2,

$u_3(t) =$ the angular acceleration, $\ddot{\theta}_3(t)$, of Link 3.

For the second manipulator, let:

$x_3(t)$ = the x-component of the position of the End-effector,

$x_4(t)$ = the y-component of the position of the End-effector,

$x_8(t)$ = the angular position, $\theta_4(t)$, of Link 4,

$x_9(t)$ = the angular position, $\theta_5(t)$, of Link 5,

$x_{10}(t)$ = the angular position, $\theta_6(t)$, of Link 6,

$x_{14}(t)$ = the angular velocity, $\dot{\theta}_4(t)$, of Link 4,

$x_{15}(t)$ = the angular velocity, $\dot{\theta}_5(t)$, of Link 5,

$x_{16}(t)$ = the angular velocity, $\dot{\theta}_6(t)$, of Link 6,

$u_4(t)$ = the angular acceleration, $\ddot{\theta}_4(t)$, of Link 4,

$u_5(t)$ = the angular acceleration, $\ddot{\theta}_5(t)$, of Link 5,

$u_6(t)$ = the angular acceleration, $\ddot{\theta}_6(t)$, of Link 6.

Then, at time t and using equation (4.2), we have (on suppressing t),

$$\left.\begin{aligned}
\dot{x}_1 &= -x_{11}x_2 - x_{12}(x_2 - l_1 \sin x_5) - x_{13} l_3 \sin(x_5 + x_6 + x_7)\,,\\
\dot{x}_2 &= x_{11}x_1 + x_{12}(x_1 - l_1 \cos x_5) + x_{13} l_3 \cos(x_5 + x_6 + x_7)\,,\\
\dot{x}_3 &= -x_{14}x_4 - x_{15}(x_4 - l_4 \sin x_8) - x_{16} l_6 \sin(x_8 + x_9 + x_{10})\,,\\
\dot{x}_4 &= x_{14}(x_3 - d) + x_{15}(x_3 - d - l_4 \cos x_8) + x_{16} l_6 \cos(x_8 + x_9 + x_{10})\,,\\
\dot{x}_5 &= x_{11}\,, \quad \dot{x}_8 = x_{14}\,, \quad \dot{x}_{11} = u_1\,, \quad \dot{x}_{14} = u_4\,,\\
\dot{x}_6 &= x_{12}\,, \quad \dot{x}_9 = x_{15}\,, \quad \dot{x}_{12} = u_2\,, \quad \dot{x}_{15} = u_5\,,\\
\dot{x}_7 &= x_{13}\,, \quad \dot{x}_{10} = x_{16}\,, \quad \dot{x}_{13} = u_3\,, \quad \dot{x}_{16} = u_6\,.
\end{aligned}\right\} \tag{4.3}$$

For cooperation, we see that the rigid object is not to be tilted at any given time t which implies that the y component of both of the End-effectors has to be same. Also, according to Figure 4.1 on page 38, the x-component of the second manipulator will be l + x-component of the first manipulator, where l is the length of the rigid object. In other words $x_4 = x_2$ and $x_3 = x_1 + l$. Thus, system (4.3) is reduced to

$$\left.\begin{aligned}
\dot{x}_1 &= -x_{11}x_2 - x_{12}(x_2 - l_1 \sin x_5) - x_{13}l_3 \sin(x_5 + x_6 + x_7)\,,\\
\dot{x}_2 &= x_{11}x_1 + x_{12}(x_1 - l_1 \cos x_5) + x_{13}l_3 \cos(x_5 + x_6 + x_7)\,,\\
\dot{x}_3 &= -x_{14}x_2 - x_{15}(x_2 - l_4 \sin x_8) - x_{16}l_6 \sin(x_8 + x_9 + x_{10})\,,\\
\dot{x}_4 &= x_{14}(x_1 + l - d) + x_{15}(x_1 + l - d - l_4 \cos x_8) + x_{16}l_6 \cos(x_8 + x_9 + x_{10})\,,\\
\dot{x}_5 &= x_{11}\,, \quad \dot{x}_8 = x_{14}\,, \quad \dot{x}_{11} = u_1\,, \quad \dot{x}_{14} = u_4\,,\\
\dot{x}_6 &= x_{12}\,, \quad \dot{x}_9 = x_{15}\,, \quad \dot{x}_{12} = u_2\,, \quad \dot{x}_{15} = u_5\,,\\
\dot{x}_7 &= x_{13}\,, \quad \dot{x}_{10} = x_{16}\,, \quad \dot{x}_{13} = u_3\,, \quad \dot{x}_{16} = u_6\,.
\end{aligned}\right\} \qquad (4.4)$$

We shall use the vector $\mathbf{x} = (x_1, ..., x_{16})$ to describe the variables in system (4.4). Also, we define the vector $\mathbf{e} = (p_1, p_2, p_3, p_2, p_5, p_6, p_7, p_8, p_9, p_{10}, 0, 0, 0, 0, 0, 0)$ where for the first manipulator, (p_1, p_2) is the final configuration of the End-effector to its target and p_5, p_6, p_7 are the angular positions of the manipulator at the target. For the second manipulator, (p_3, p_2) is the final configuration of the End-effector to its target and p_8, p_9, p_{10} are the angular positions of the manipulator at the target.

4.4 Target

We define the targets of the manipulators as the points (p_1, p_2) and (p_3, p_4). Now, we want to have a kind of a yardstick that measures, at time t, the position of the End-effectors from the points (p_1, p_2) and (p_3, p_2) and the rate at which it approaches or moves away from (p_1, p_2) and (p_3, p_2). The following choice of probable functions accomplishes this (on suppressing t).

$$V_0(\mathbf{x}) = \frac{1}{2}\left[(x_1 - p_1)^2 + (x_2 - p_2)^2 + (x_1 + l - p_3)^2 + x_{11}^2 + x_{12}^2 + x_{13}^2 + x_{14}^2 + x_{15}^2 + x_{16}^2\right],$$

noting that $V_0(\mathbf{e}) = 0$ and $V_0 \geq 0$ for $\mathbf{x} \neq \mathbf{e}$.

4.5 Antitarget

4.5.1 Singular Configurations

The singular configurations occur when $\theta_2 = x_4 = 0, \pi$, $\theta_3 = x_5 = 0, \pi$, $\theta_5 = x_9 = 0, \pi$ and $\theta_6 = x_{10} = 0, \pi$ in the anticlockwise direction or $\theta_2 = x_4 = -\pi$, $\theta_3 = x_5 = -\pi$, $\theta_5 = x_9 = -\pi$, $\theta_6 = x_{10} = -\pi$ in the clockwise direction. For the configuration, consider the functions

$$W_1(x) = |x_6|, W_2(x) = \pi - |x_6|, W_3(x) = |x_7|, W_4(x) = \pi - |x_7|,$$

$$W_5(x) = |x_9|, W_6(x) = \pi - |x_9|, W_7(x) = |x_{10}|, W_8(x) = \pi - |x_{10}|$$

for $x_6, x_7, x_9,\, x_{10} \in (-\pi, \pi) \cup (0, \pi)$.

4.5.2 Obstacle Avoidance and Target Attraction

The Lyapunov function of our system must be exactly zero at the target center. Consequently we introduce:

$$F_3(\mathbf{x}) = \frac{1}{2}\left[(x_1 - p_1)^2 + (x_2 - p_2)^2 + (x_1 + l - p_3)^2\right] \geq 0$$

4.5.3 A Lyapunov Function

Consider the tentative Lyapunov function,

$$V(\mathbf{x}) = V_0(\mathbf{x}) + F_3(\mathbf{x}) \sum_{i=1}^{8} \frac{\beta_i}{W_i}$$

where β_i is a positive constant. Clearly, V is continuous and positive on the domain $\mathbb{D}(V) = \{x \in \mathbf{R}^{16} : W_i > 0, i = 1, ..., 8\}$.

Along a particular trajectory of system (4.4), we have (on suppressing t),

$$\begin{aligned} \dot{V}(\mathbf{x}) &= \dot{V}_0(\mathbf{x}) + \dot{F}_3(\mathbf{x}) \sum_{i=1}^{8} \frac{\beta_i}{W_i} - F_3(\mathbf{x}) \sum_{i=1}^{8} \frac{\beta_i \dot{W}_i}{W_i^2} \\ &= \{G_1 + u_1\}x_{11} + \{G_2 + u_2\}x_{12} + \{G_3 + u_3\}x_{13} \\ &+ u_4 x_{14} + \{G_5 + u_5\}x_{15} + \{G_6 + u_6\}x_{16} \end{aligned}$$

where $G_1, G_2, ..., G_6$ are defined in Appendix A.4.

Also, we see that for $\mathbf{e} = (p_1, p_2, p_3, p_2, p_5, p_6, p_7, p_8, p_9, p_{10}, 0, 0, 0, 0, 0, 0)$, we have $V(\mathbf{e})$ $= \mathbf{0}$, and since $\mathbf{e} \in \mathbb{D}(V)$, we may take $\mathbb{D}(V)$ as the neighbourhood $\mathbb{D}$ of the point $\mathbf{e}$. Now, for some numbers $\alpha_1 > 0$, $\alpha_2 > 0$, $\alpha_3 > 0$, $\alpha_4 > 0$, $\alpha_5 > 0$ and $\alpha_6 > 0$, define $-\alpha_1 x_{11} = G_1 + u_1$, $-\alpha_2 x_{12} = G_2 + u_2$, $-\alpha_3 x_{13} = G_3 + u_3$, $-\alpha_4 x_{14} = u_4$, $-\alpha_5 x_{15} = G_5 + u_5$ and $-\alpha_6 x_{16} = G_6 + u_6$.

Then

$$\dot{V}(\mathbf{x}) = -\alpha_1 x_{11}^2 - \alpha_2 x_{12}^2 - \alpha_3 x_{13}^2 - \alpha_4 x_{14}^2 - \alpha_5 x_{15}^2 - \alpha_6 x_{16}^2 \leq 0,$$

provided we have $u_1 = -\alpha_1 x_{11} - G_1$, $u_2 = -\alpha_2 x_{12} - G_2$, $u_3 = -\alpha_3 x_{13} - G_3$, $u_4 = -\alpha_4 x_{14}$, $u_5 = -\alpha_5 x_{15} - G_5$, and $u_6 = -\alpha_6 x_{16} - G_6$ as the *nonlinear controllers*. Since $\dot{V}(\mathbf{x})$ is nonpositive and continuous for all $\mathbf{x} \in \mathbb{D}(V)$, by Lyapunov's stability Theorem 1.5.1, V is a Lyapunov function for system (4.4) on $\mathbb{D}(V)$ establishing the stability of $\mathbf{e}$. Hence,

e is an equilibrium point of system (4.4), and our Lyapunov function satisfies Theorem 1.5.1 at this equilibrium point.

Thus, we have the system

$$\left.\begin{aligned}
\dot{x}_1 &= -x_{11}x_2 - x_{12}(x_2 - l_1 \sin x_5) - x_{13}l_3 \sin(x_5 + x_6 + x_7)\,,\\
\dot{x}_2 &= x_{11}x_1 + x_{12}(x_1 - l_1 \cos x_5) + x_{13}l_3 \cos(x_5 + x_6 + x_7)\,,\\
\dot{x}_3 &= -x_{14}x_2 - x_{15}(x_2 - l_4 \sin x_8) - x_{16}l_6 \sin(x_8 + x_9 + x_{10})\,,\\
\dot{x}_4 &= x_{14}(x_1 + l - d) + x_{15}(x_1 + l - d - l_4 \cos x_8) + x_{16}l_6 \cos(x_8 + x_9 + x_{10})\,,\\
\dot{x}_5 &= x_{11}\,, \quad \dot{x}_8 = x_{14}\,, \quad \dot{x}_{11} = \alpha_1 x_{11} - G_1\,, \quad \dot{x}_{14} = -\alpha_4 x_{14}\,,\\
\dot{x}_6 &= x_{12}\,, \quad \dot{x}_9 = x_{15}\,, \quad \dot{x}_{12} = -\alpha_2 x_{12} - G_2\,, \quad \dot{x}_{15} = -\alpha_5 x_{15} - G_5\,,\\
\dot{x}_7 &= x_{13}\,, \quad \dot{x}_{10} = x_{16}\,, \quad \dot{x}_{13} = -\alpha_3 x_{13} - G_3\,, \quad \dot{x}_{16} = -\alpha_6 x_{16} - G_6\,,
\end{aligned}\right\} \quad (4.5)$$

which is stable at the equilibrium point $\mathbf{e} = (p_1, p_2, p_5, p_6, p_7, p_8, p_9, p_{10}, 0, 0, 0, 0, 0, 0)$.

4.6 A Computer Simulation

The computer is used to numerically integrate system (4.5) to obtain the solution $(x_1, ..., x_{16})$ and plot the points $(x_1(t), x_2(t))$, $(x_1(t) + l, x_2(t))$ at time t in the x_1x_2-plane until the points converge to a neighbourhood of (p_1, p_2), (p_3, p_2), respectively and stay there as $t \to \infty$. For our example, Table 4.1 on page 46 gives the parameters, and Figure 4.2 on page 45 gives the trajectory of the arm. Notice the slowing down of the arm as it approaches to its final configuration. This could be explained in terms of the potential energy "cup" of the Lyapunov function derived by Vanualailai and Bibhya [15]. The arm reaches its final configuration in about 10 units of time.

Figure 4.3 on page 47 shows the behaviour of the controllers for the first manipulator, that is the controllers u_1 (dashed line), u_2 (bold line) and u_3 (solid line) which converge

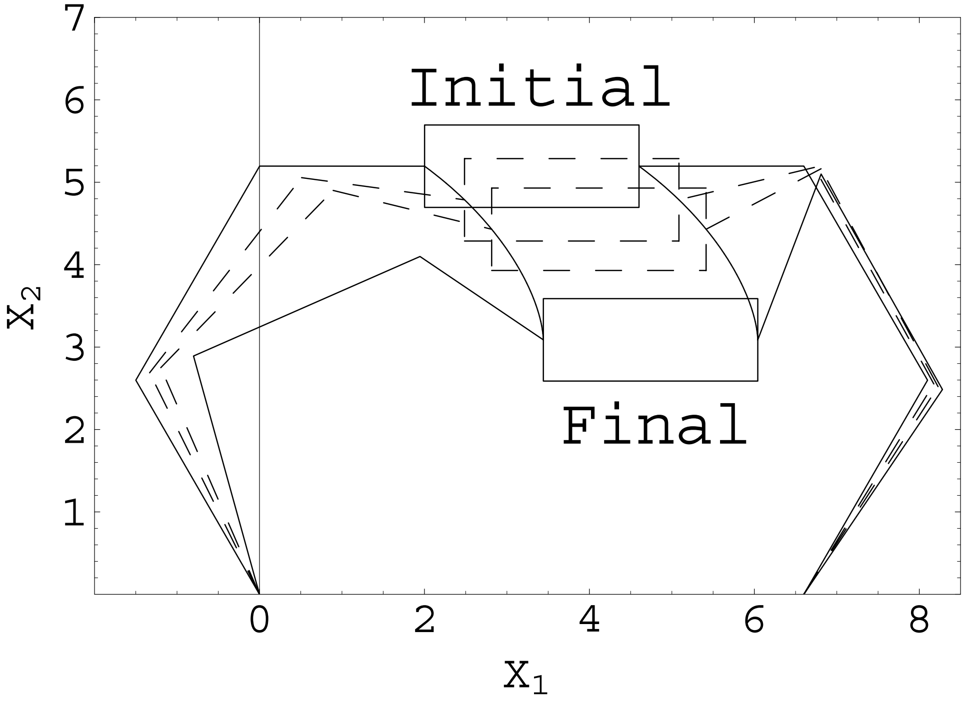

Figure 4.2: Animation of the motion of the dual-arm cooperative manipulators.

Table 4.1: A Scenario 1 example.

Lengths of Links	$l_1 = 3, l_2 = 3, l_3 = 2, l_4 = 3,$ $l_5 = 3$ and $l_6 = 2$
Initial Conditions	$\mathbf{x} = (2, 5.196, 4.6, 5.196, 2\pi/3, -\pi/3, \pi/3,$ $\pi/3, \pi/3, \pi/180, \pi/180, \pi/180,$ $\pi/180, \pi/180, \pi/180)$
Planar Target	$(p_1, p_2) = (3.44, 3)$ and $(p_3, p_2) = (6.04, 3)$
Control Parameters	$\beta_1 = \beta_2 = \beta_3 = \beta_4 = 0.01$ and $\beta_5 = \beta_6 = \beta_7 = \beta_8 = 0.01$
Convergence Parameters	$\alpha_1 = 150, \alpha_2 = 150, \alpha_3 = 150,$ $\alpha_4 = 0.05, \alpha_5 = 150$ and $\alpha_6 = 150$
Length of the rigid object	$l = 2.6$

to 0 as time $t \to \infty$. Figure 4.4 on page 47 shows the behaviour of the controllers for the second manipulator, that is the controllers u_4 (dashed line), u_5 (bold line) and u_6 (solid line) which converge to 0 as time $t \to \infty$.

4.6.1 Remark

Under the proposed controllers, we saw that dual-arm cooperative manipulators reached their targets safely having a smooth trajectory.

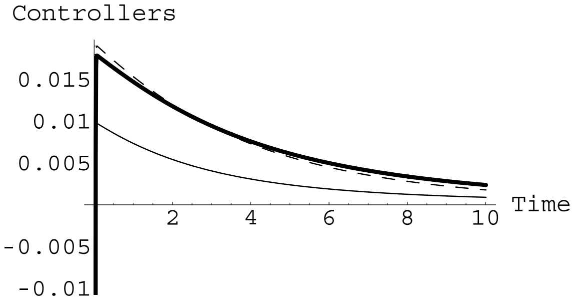

Figure 4.3: Behaviour of the nonlinear controllers; u_1 (dashed line), u_2 (bold line) and u_3 (solid line).

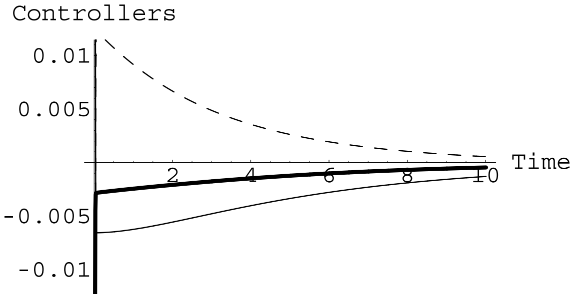

Figure 4.4: Behaviour of the nonlinear controllers; u_4 (dashed line), u_5 (bold line) and u_6 (solid line).

Chapter 5

A differential Drive Mobile Manipulator

5.1 Introduction

A kinematic motion planning methodology is developed for a differential drive mobile manipulator using geometry. The method constructs trajectory inputs that drive both the manipulator and its platform to a final configuration without violating the nonholonomic constraints.

The controllers for the system are extracted from Lyapunov's second method which inherently ensures stability. We propose smooth control laws to control the motion of the mobile manipulator system on a differentially-driven platform. We design a specific scenario and the results obtained illustrate the effectiveness of the controllers. Finally, we look at real life situations where differential drive mobile manipulators can be used.

5.2 Nonholonomic Mobile Platform System

We consider the mobile manipulator system as depicted in Figure 5.1 below.

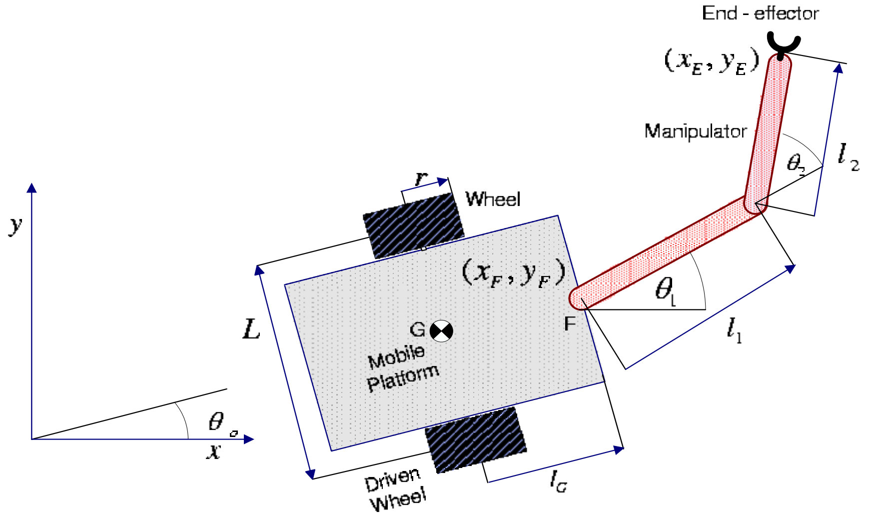

Figure 5.1: Schematic representation of the mobile manipulator system on a differentially-driven platform.

The reference point is the midpoint of the axle (length L) joining the two wheels, with θ

as the direction of the travel. The dynamic model is given as:

$$\dot{x}_G = \frac{1}{2}\{\upsilon_1 + \upsilon_2\}\cos\theta_0$$

$$\dot{y}_G = \frac{1}{2}\{\upsilon_1 + \upsilon_2\}\sin\theta_0$$

$$\dot{\theta}_0 = \frac{1}{L}\{\upsilon_1 - \upsilon_2\} = \omega$$

$$\dot{\upsilon}_1 = \mu_1$$

$$\dot{\upsilon}_2 = \mu_2$$

where μ_1 and μ_2 are bound and where υ_1 and υ_2 are the wheel velocities which are themselves bounded. Because of no lateral movement of the wheels, the lateral velocity is zero, giving us the nonholonomic constraint

$$\dot{x}_G \sin\theta_0 - \dot{y}_G \cos\theta_0 = 0. \tag{5.1}$$

Now, for the manipulator attachment point F, the equation is as follows:

$$\dot{x}_F \sin\theta_0 - \dot{y}_F \cos\theta_0 + \omega\theta_0 l_G = 0, \tag{5.2}$$

where l_G is the distance between G and F. Due to the nature of this constraint, the planning must be designed at the differential kinematics level. In general, the above is the equation of motion of the platform only. Now we consider the manipulator and the platform. Letting $\alpha = \theta_0 + \theta_1 + \theta_2$, the position and the configuration of the End-effector can be written as follows:

$$\left.\begin{aligned} x_E(t) &= x_G(t) + l_G\cos\theta_0(t) + l_1\cos(\theta_0(t) + \theta_1(t)) + l_2\cos\alpha\,, \\ y_E(t) &= y_G(t) + l_G\sin\theta_0(t) + l_1\sin(\theta_0(t) + \theta_1(t)) + l_2\sin\alpha\,. \end{aligned}\right\} \tag{5.3}$$

The instantaneous velocities (on suppressing t) are:

$$\left.\begin{aligned} \dot{x}_E &= \dot{x}_G - \omega l_G\sin\theta_0 + (\omega - \dot{\theta}_1)l_1\sin(\theta_0 + \theta_1) - \dot{\alpha}l_2\sin\alpha\,, \\ \dot{y}_E &= \dot{y}_G - \omega l_G\cos\theta_0 + (\omega + \dot{\theta}_1)l_1\cos(\theta_0 + \theta_1) + \dot{\alpha}l_2\cos\alpha\,. \end{aligned}\right\} \tag{5.4}$$

The above equations can further be written as:

$$\left.\begin{array}{rcl} \dot{x}_E(t) & = & \frac{1}{2}\upsilon_1\cos\theta_0 + \frac{1}{2}\upsilon_2\cos\theta_0 - \omega l_G\sin\theta_0 \\ & + & (-\omega - \dot{\theta}_1)l_1\sin(\theta_0+\theta_1) - \dot{\alpha}l_2\sin\alpha\,, \\ \dot{y}_E(t) & = & \frac{1}{2}\upsilon_1\sin\theta_0 + \frac{1}{2}\upsilon_2\sin\theta_0 + \omega l_G\cos\theta_0 \\ & + & (\omega + \dot{\theta}_1)l_1\cos(\theta_0+\theta_1) + \dot{\alpha}l_2\cos\alpha\,. \end{array}\right\} \tag{5.5}$$

5.3 Kinematic Modelling

We state a system of first-order differential equations describing the motion of the differential drive mobile manipulator.

For the manipulator, let:

$x_1(t)$ = the x-component of the position of the End-effector,

$x_2(t)$ = the y-component of the position of the End-effector,

$x_4(t)$ = the angular position, $\theta_1(t)$, of Link 1,

$x_5(t)$ = the angular position, $\theta_2(t)$, of Link 2,

$x_9(t)$ = the angular velocity, $\dot{\theta}_1(t)$, of Link 1,

$x_{10}(t)$ = the angular velocity, $\dot{\theta}_2(t)$, of Link 2,

$u_4(t)$ = the angular acceleration, $\ddot{\theta}_1(t)$, of Link 1,

$u_5(t)$ = the angular acceleration, $\ddot{\theta}_2(t)$, of Link 2.

For the platform, let:

$x_3(t)$ = the angular position, $\theta_0(t)$, of platform,

$x_6(t)$ = the linear velocity of the right wheel,

$x_7(t)$ = the linear velocity of the left wheel,

$x_8(t)$ = the angular velocity, $\dot{\theta}_0(t)$, of platform,

$u_1(t) =$ the linear acceleration of the right wheel

$u_2(t) =$ the linear acceleration of the left wheel

$u_3(t) =$ the angular acceleration, $\ddot{\theta}_0(t)$, of platform,

Then at time t and using equation (5.5), we have (on suppressing t),

$$\left.\begin{aligned}
\dot{x}_1 &= \tfrac{1}{2}(x_6 + x_7)\cos x_3 - x_8 l_G \sin x_3 - x_8 l_1 \sin(x_3 + x_4) - x_9 l_1 \sin(x_3 + x_4) \\
&\quad - x_8 l_2 \sin(x_3 + x_4 + x_5) - x_9 l_2 \sin(x_3 + x_4 + x_5) - x_{10} l_2 \sin(x_3 + x_4 + x_5)\,, \\
\dot{x}_2 &= \tfrac{1}{2}(x_6 + x_7)\sin x_3 + x_8 l_G \cos x_3 + x_8 l_1 \cos(x_3 + x_4) + x_9 l_1 \cos(x_3 + x_4) \\
&\quad + x_8 l_2 \cos(x_3 + x_4 + x_5) + x_9 l_2 \cos(x_3 + x_4 + x_5) + x_{10} l_2 \cos(x_3 + x_4 + x_5)\,, \\
\dot{x}_3 &= x_8\,, \qquad \dot{x}_6 = u_1\,, \qquad \dot{x}_9 = u_4\,, \\
\dot{x}_4 &= x_9\,, \qquad \dot{x}_7 = u_2\,, \qquad \dot{x}_{10} = u_5\,, \\
\dot{x}_5 &= x_{10}\,, \qquad \dot{x}_8 = u_3\,.
\end{aligned}\right\} \tag{5.6}$$

We shall use the vector $\mathbf{x} = (x_1, ..., x_{10})$ to describe the variables in system (5.6). Also, we define the vector $\mathbf{e} = p_1, p_2, p_3, p_4, p_5, 0, 0, 0, 0, 0, 0)$. Here, we define (p_1, p_2) as the final configuration of the end-effector at the target, p_3 as the angular position of the platform at the target, p_4, p_5 as the angular positions of the arm at the target.

5.4 Avoidance Functions

5.4.1 Avoidance of Singular Configurations.

The singular configurations occur when $\theta_2 = x_5 = 0, \pi$ in the anticlockwise direction or $\theta_2 = x_5 = -\pi$ in the clockwise direction. For the configuration, consider the functions

$$W_1(\mathbf{x}) = |x_5|$$

and

$$W_2(\mathbf{x}) = \pi - |x_5|,$$

for $x_5 \in (-\pi, 0) \cup (0, \pi)$.

5.5 Target Attraction and Obstacle Avoidance

The Lyapunov function of our system must be exactly zero at the target center. Consequently we introduce:

$$F_0(\mathbf{x}) = \frac{1}{2}\left[(x_1 - p_1)^2 + (x_2 - p_2)^2\right] \geq 0$$

5.5.1 A Lyapunov Function

Consider the tentative Lyapunov function,

$$V(\mathbf{x}) = V_0(\mathbf{x}) + F(\mathbf{x}) \sum_{i=1}^{2} \frac{\beta_i}{W_i(\mathbf{x})}$$

where β_i is a positive constant and

$$V_0(\mathbf{x}) = \frac{1}{2}\left[(x_1 - p_1)^2 + (x_2 - p_2)^2 + x_6^2 + x_7^2 + x_8^2 + x_9^2 + x_{10}^2\right].$$

Clearly, V is continuous and positive on the domain

$$\mathbb{D}(V) = \{\mathbf{x} \in \mathbf{R}^{10} : W_i > 0, i = 1, 2\}.$$

Along a particular trajectory of system (5.6), we have (on suppressing t),

$$\begin{aligned} \dot{V}(\mathbf{x}) &= \dot{V}_0(\mathbf{x}) + \dot{F}(\mathbf{x}) \sum_{i=1}^{2} \frac{\beta_i}{W_i} - F(\mathbf{x}) \sum_{i=1}^{2} \frac{\beta_i \dot{W}_i}{W_i^2} \\ &= \{G_1(\mathbf{x}) + u_1\}x_6 + \{G_2(\mathbf{x}) + u_2\}x_7 + \{G_3(\mathbf{x}) + u_3\}x_8 \\ &\quad + \{G_4(\mathbf{x}) + u_4\}x_9 + \{G_5(\mathbf{x}) + u_5\}x_{10} \end{aligned}$$

where G_1, G_2, G_3 and G_4 are defined in Appendix A.5. Also, we see that for $\mathbf{e} = p_1, p_2, p_3, p_4, p_5, 0, 0, 0, 0, 0, 0)$, we have $V(\mathbf{e}) = \mathbf{0}$, and since $\mathbf{e} \in \mathbb{D}(V)$, we may take $\mathbb{D}(V)$ as the neighbourhood $\mathbb{D}$ of the point $\mathbf{e} = (p_1, p_2, p_3, p_4, p_5, 0, 0, 0, 0, 0, 0)$.

For some numbers $\alpha_1 > 0$, $\alpha_2 > 0$, $\alpha_3 > 0$, $\alpha_4 > 0$ and $\alpha_5 > 0$, define $-\alpha_1 x_6 = G_1 + u_1$, $-\alpha_2 x_7 = G_2 + u_2$, $-\alpha_3 x_8 = G_3 + u_3$, $-\alpha_4 x_9 = G_4 + u_4$ and $-\alpha_5 x_{10} = G_5 + u_5$.

Then

$$\dot{V}(\mathbf{x}) = -\alpha_1 x_6^2 - \alpha_2 x_7^2 - \alpha_3 x_8^2 - \alpha_4 x_9^2 - \alpha_5 x_{10}^2 \leq 0,$$

provided we have $u_1 = -\alpha_1 x_6 - G_1$, $u_2 = -\alpha_2 x_7 - G_2$, $u_3 = -\alpha_3 x_8 - G_3$, $u_4 = -\alpha_4 x_9 - G_4$ and $u_5 = -\alpha_5 x_{10} - G_5$ as the *nonlinear controllers*. Since $\dot{V}(\mathbf{x})$ is nonpositive and continuous for all $\mathbf{x} \in \mathbb{D}(V)$, by Lyapunov's stability Theorem 1.5.1, V is a Lyapunov function for system (5.6) on $\mathbb{D}(V)$ establishing the stability of $\mathbf{e}$. Hence, $\mathbf{e}$ is an equilibrium point of system (5.6), and our Lyapunov function satisfies Theorem 1.5.1 at this equilibrium point.

Thus, we have the system

$$\left.\begin{aligned}
\dot{x}_1 &= \tfrac{1}{2}(x_6 + x_7)\cos x_3 - x_8 l_G \sin x_3 - x_8 l_1 \sin(x_3 + x_4) - x_9 l_1 \sin(x_3 + x_4) \\
&\quad -x_8 l_2 \sin(x_3 + x_4 + x_5) - x_9 l_2 \sin(x_3 + x_4 + x_5) - x_{10} l_2 \sin(x_3 + x_4 + x_5)\,, \\
\dot{x}_2 &= \tfrac{1}{2}(x_6 + x_7)\sin x_3 + x_8 l_G \cos x_3 + x_8 l_1 \cos(x_3 + x_4) + x_9 l_1 \cos(x_3 + x_4) \\
&\quad +x_8 l_2 \cos(x_3 + x_4 + x_5) + x_9 l_2 \cos(x_3 + x_4 + x_5) + x_{10} l_2 \cos(x_3 + x_4 + x_5)\,, \\
\dot{x}_3 &= x_8\,, \qquad \dot{x}_6 = -\alpha_1 x_6 - G_1\,, \qquad \dot{x}_9 = -\alpha_4 x_9 - G_4\,, \\
\dot{x}_4 &= x_9\,, \qquad \dot{x}_7 = -\alpha_1 x_6 - G_2\,, \qquad \dot{x}_{10} = -\alpha_5 x_{10} - G_5\,, \\
\dot{x}_5 &= x_{10}\,, \qquad \dot{x}_8 = -\alpha_3 x_8 - G_3\,,
\end{aligned}\right\} \tag{5.7}$$

which is stable at the equilibrium point $\mathbf{e} = (p_1, p_2, p_3, p_4, p_5, 0, 0, 0, 0, 0, 0)$.

5.6 A Computer Simulation

The computer is used to numerically integrate system (5.7) to obtain the solution $(x_1, ..., x_{10})$ and plot the points $(x_1(t), x_2(t))$ at time t in the x_1x_2-plane until the points converge to a neighbourhood of (p_1, p_2) and stay there as $t \to \infty$. Table 5.1 below gives the parameters, and Figure 5.2 below on page 57 gives the trajectory of the arm while Table 5.2 on page 56 gives the parameters, and Figure 5.6 on page 59 gives the trajectory of the arm for Scenario 1 example and Scenario 2 example respectively. Notice the slowing down of the mobile manipulator as it approaches its final configuration. This could be explained in terms of the potential energy "cup" of the Lyapunov function derived by Vanualailai and Bibhya [15]. The arm reaches its final configuration in about 10 units of time. In Figure 5.6 on page 59, the first five links are drawn every 0.02 unit of time.

Table 5.1: A Scenario 1 example.

Lengths of Links	$l_1 = 2$, and $l_2 = 2$
Initial Conditions	$\mathbf{x} = (12.63854, 8.793155, \pi/6, \pi/3, -2\pi/3, 550, 650, 3\pi, \pi/180, \pi/180)$
Planar Target	$(p_1, p_2) = (6, 10)$
Control Parameters	$\beta_1 = 30$ and $\beta_2 = 40$
Convergence Parameters	$\alpha_1 = 150, \alpha_2 = 150, \alpha_3 = 100, \alpha_4 = 100$ and $\alpha_5 = 100$

Table 5.2: A Scenario 2 example.

Lengths of Links	$l_1 = 2$, and $l_2 = 2$
Initial Conditions	$\mathbf{x} = (10.4, 6.5, \pi/6, \pi/3, -2\pi/3, 650, 550, 3\pi, \pi/180, \pi/180)$
Planar Target	$(p_1, p_2) = (15, 15)$
Control Parameters	$\beta_1 = 0.01$ and $\beta_2 = 0.01$
Convergence Parameters	$\alpha_1 = \alpha_2 = \alpha_3 = \alpha_4 = \alpha_5 = 50$

Figure 5.2 and Figure 5.6 on pages 57 and 59 present snapshots of the motion of the differential drive mobile manipulator for Scenario 1 example and Scenario 2 example respectively. The given path for the End-effector (solid line) and the front point of the platform (dashed line) are shown in Figure 5.3 on page 58. In Figure 5.4 on page 58, u_1 (dashed line), u_2 (bold line) and in Figure 5.5 on page 59, u_3 (dashed line), u_4 (bold line) and u_5 (solid line) show the behaviour of the controllers along the trajectory of the differential drive manipulator. It can be seen that the controllers converge to 0 as time $t \to \infty$.

5.6.1 Remark

Under the proposed controllers, we saw that the differential drive manipulator reached the target safely having a smooth trajectory in both of the examples. The differential drive mobile manipulator behaves similar to wheel chairs. It can act as an assistance device for handicapped people in manipulating and moving an object. The disabled person feels involved in the service given by this manipulator system and is no more completely dependent.

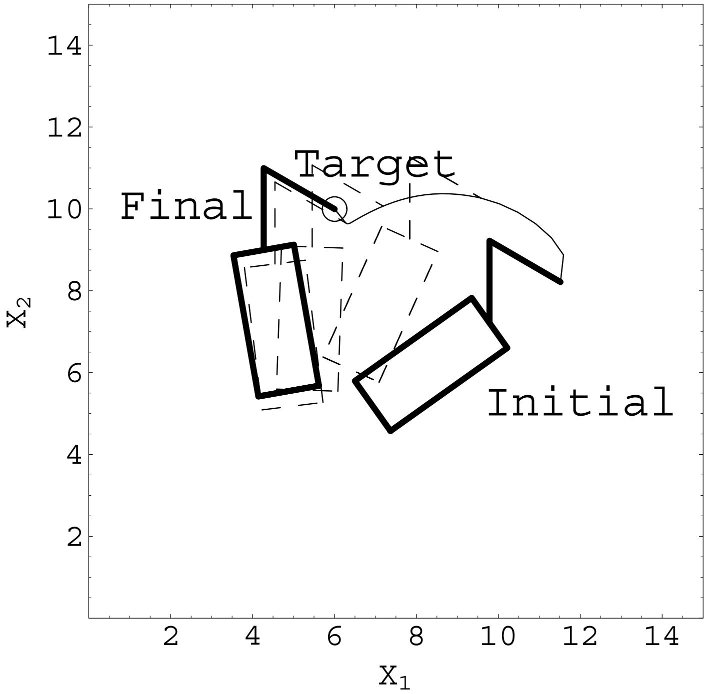

Figure 5.2: Animation of the motion of the mobile manipulator with a differential drive.

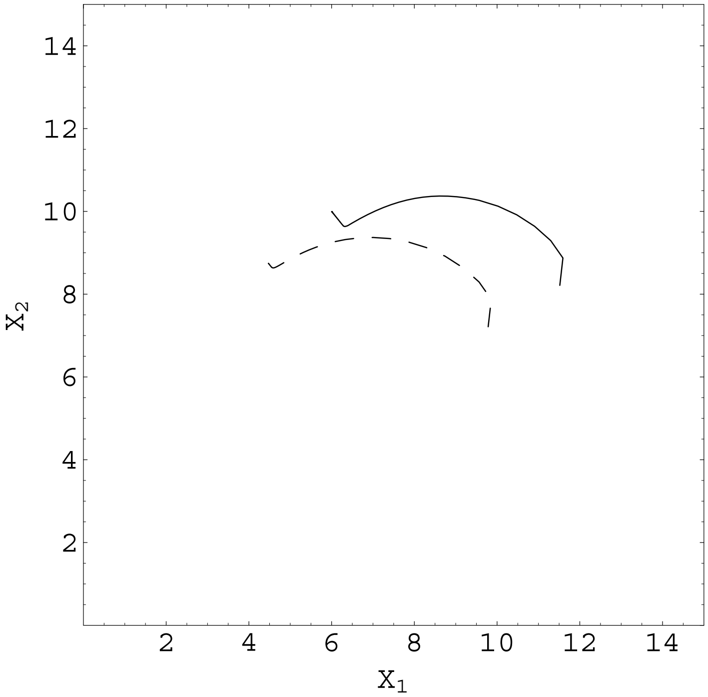

Figure 5.3: Desired platform and End-effector path.

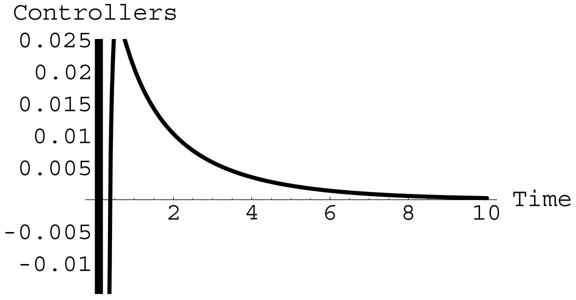

Figure 5.4: Behaviour of the nonlinear controllers; u_1 (dashed line), u_2 (bold line).

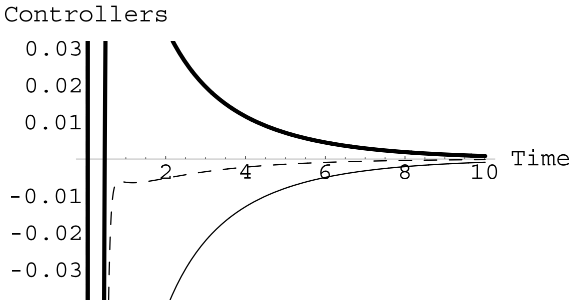

Figure 5.5: Behaviour of the nonlinear controllers; u_3 (dashed line) and u_4 (bold line).

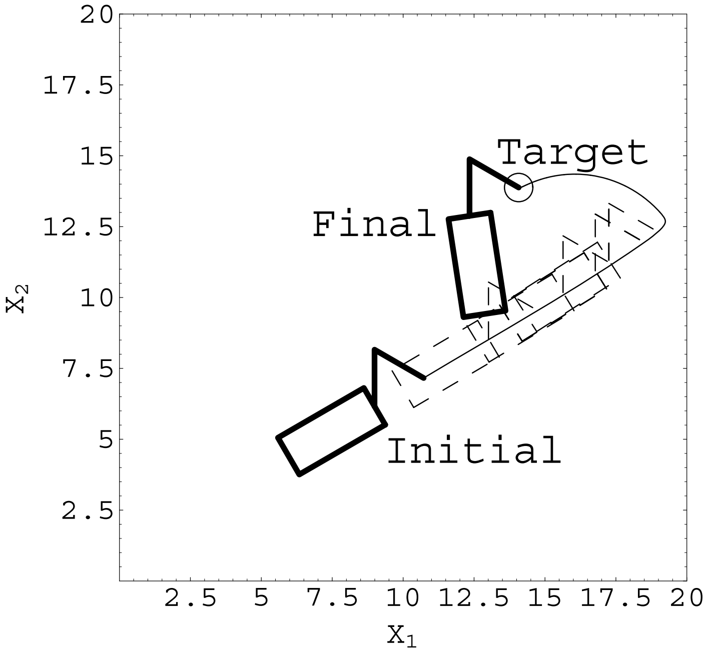

Figure 5.6: Animation of the motion of the mobile manipulator with a differential drive.

Chapter 6

A Car-like Mobile Manipulator

6.1 Introduction

We consider a simple mobile manipulator system whose platform includes front and rear wheels and derive its kinematic equation of motion using geometry.

We use Lyapunov's second method to extract controllers which inherently ensures stability to control the motion of a car-like mobile manipulator. We consider a specific scenario and the results obtained illustrate the effectiveness of the controllers. Finally, we look at real life situations where car-like mobile manipulators can be used.

6.2 Nonholonomic Rover System

We will consider a car-like manipulator whose platform includes a steering wheel and two fixed rear wheels as shown in Figure 6.1 below.

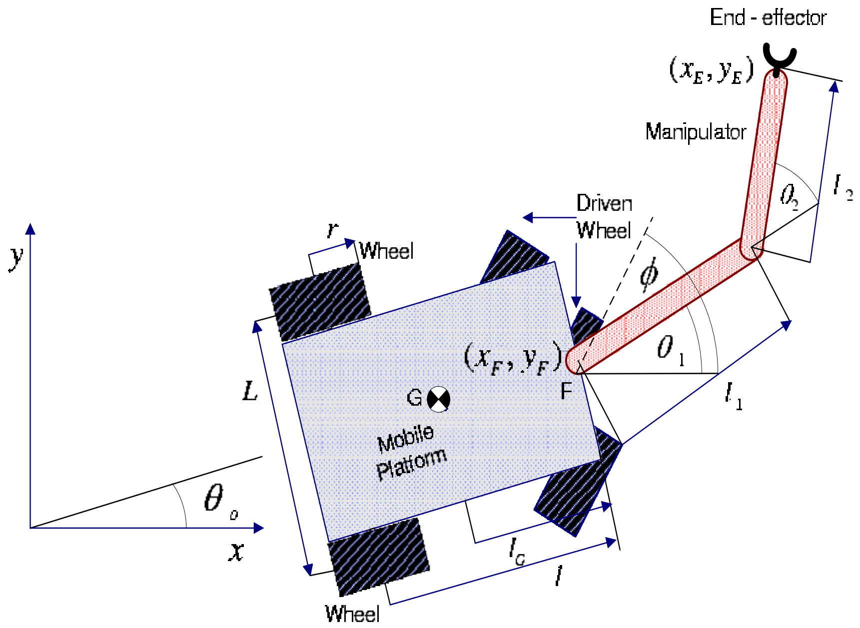

Figure 6.1: Schematic representation of the car-like mobile manipulator system.

The exact configuration of our car-like vehicle can be described by 4 variables. We start by specifying a frame of reference, in which an arbitrarily chosen point is treated as stationary. Thus, all other points are treated to be moving with respect to the nominated reference point. The (x, y) coordinates gives the location of the center of the rear axle and this is our reference point. θ gives the car's angle with respect to the x-axis, while ϕ gives the steering wheel's angle with respect to the car's longitudinal axis. We should also remember that this steering angle is physically limited to $|\phi| \leq \phi_{max}$.

Let us consider the nonholonomic constraints for the rear wheels. The velocity perpendicular to the linear velocity of the car is zero because of no slippage. The linear velocity with respect to the rear axle is denoted as υ. The slope of the velocity at the center of the rear axle is then zero, from which we get our first equation for the nonholonomic constraints:

$$\dot{x} \sin \theta_0 - \dot{y} \cos \theta_0 = 0. \tag{6.1}$$

Similarly, for the front wheels:

$$\dot{\upsilon}_2 = \frac{\dot{y}_F}{\dot{x}_F} = \frac{\upsilon_2 \cos(\theta_0 + \phi)}{\upsilon_2 \sin(\theta_0 + \phi)} = 0, \tag{6.2}$$

from which we get our second equation for the nonholonomic constraints:

$$\dot{x}_F \sin(\theta_0 + \phi) - \dot{y}_F \cos(\theta_0 + \phi) = 0. \tag{6.3}$$

The velocity of the car with respect to the x and y directions is then given as:

$$\dot{x} = \upsilon \cos \theta_0,$$

$$\dot{y} = \upsilon \sin \theta_0.$$

Now, the location of the center of the front axle is then given as:

$$x_F = x + l \cos \theta_0,$$

$$y_F = x + l \sin \theta_0.$$

The velocity is then:

$$\dot{x}_F = \dot{x} - l \sin \theta_0 * \dot{\theta}_0,$$

$$\dot{y}_F = \dot{y} + l \cos \theta_0 * \dot{\theta}_0.$$

Now suppose we want to use the same system but the reference point as the center of the car, then we will have to take the mid-point of the front and rear axis. Thus, we have

$$x_E = \frac{1}{2}\{x_r + x_F\},$$

$$y_E = \frac{1}{2}\{y_r + y_F\},$$

which after differentiation becomes

$$\dot{x}_E = \frac{1}{2}\{\dot{x}_r + \dot{x}_F\},$$

$$\dot{y}_E = \frac{1}{2}\{\dot{y}_r + \dot{y}_F\}.$$

Now carrying out the substitutions from the equations above:

$$\dot{x}_E = \frac{1}{2}\{\upsilon \cos \theta_0 + \{\upsilon \cos \theta_0 - l\dot{\theta}_0 \sin \theta_0\}\} = \upsilon \cos \theta_0 - \frac{l}{2}\dot{\theta}_0 \sin \theta_0$$

$$\dot{y}_E = \frac{1}{2}\{\upsilon \sin \theta_0 + \{\upsilon \sin \theta_0 + l\dot{\theta}_0 \cos \theta_0\}\} = \upsilon \sin \theta_0 + \frac{l}{2}\dot{\theta}_0 \cos \theta_0$$

thus, the kinematic model of the vehicle with respect to the center with $\phi = \theta$, is given as:

$$\dot{x} = \upsilon \cos \theta_0 - \frac{l}{2}\dot{\theta}_0 \sin \theta_0 = \upsilon \cos \theta_0 - \frac{l}{2}\omega \sin \theta_0$$

$$\dot{y} = \upsilon \sin \theta_0 + \frac{l}{2}\dot{\theta}_0 \cos \theta_0 = \upsilon \sin \theta_0 + \frac{l}{2}\omega \cos \theta_0$$

$$\dot{\theta}_0 = \frac{\upsilon}{l} \tan \theta = \omega$$

Now we consider the manipulator and the platform. The position and the configuration of the End-effector can be written as follows:

$$\left.\begin{aligned} x_E(t) &= x(t) + \tfrac{l}{2}\cos\theta_0(t) + l_1\cos(\theta_0(t)+\theta_1(t)) \\ &+ l_2\cos(\theta_0(t)+\theta_1(t)+\theta_2(t))\,, \\ y_E(t) &= y(t) + \tfrac{l}{2}\sin\theta_0(t) + l_1\sin(\theta_0(t)+\theta_1(t)) \\ &+ l_2\sin(\theta_0(t)+\theta_1(t)+\theta_2(t))\,. \end{aligned}\right\} \tag{6.4}$$

The instantaneous velocities (on suppressing t) are:

$$\left.\begin{aligned} \dot{x}_E &= \dot{x} - \omega\tfrac{l}{2}\sin\theta_0 - (\omega+\dot{\theta}_1)l_1\sin(\theta_0+\theta_1) \\ &- (\omega+\dot{\theta}_1+\dot{\theta}_2)l_2\sin(\theta_0+\theta_1+\theta_2)\,, \\ \dot{y}_E &= \dot{y} + \omega\tfrac{l}{2}\cos\theta_0 + (\omega+\dot{\theta}_1)l_1\sin(\theta_0+\theta_1) \\ &+ (\omega+\dot{\theta}_1+\dot{\theta}_2)l_2\cos(\theta_0+\theta_1+\theta_2)\,. \end{aligned}\right\} \tag{6.5}$$

The above equations can further be written as:

$$\left.\begin{aligned} \dot{x}_E &= v\cos\theta_0 - l\omega\sin\theta_0 - (\omega+\dot{\theta}_1)l_1\sin(\theta_0+\theta_1) \\ &- (\omega+\dot{\theta}_1+\dot{\theta}_2)l_2\sin(\theta_0+\theta_1+\theta_2)\,, \\ \dot{y}_E &= v\sin\theta_0 + l\omega\cos\theta_0 + (\omega+\dot{\theta}_1)l_1\sin(\theta_0+\theta_1) \\ &+ (\omega+\dot{\theta}_1+\dot{\theta}_2)l_2\cos(\theta_0+\theta_1+\theta_2)\,. \end{aligned}\right\} \tag{6.6}$$

6.3 Kinematic Modelling

We state a system of first-order differential equations describing the motion of the car-like differential drive mobile manipulator. For the manipulator, let:

$x_1(t) =$ the x-component of the position of the End-effector,

$x_2(t) =$ the y-component of the position of the End-effector,

$x_4(t) =$ the angular position, $\theta_1(t)$, of Link 1,

$x_5(t) =$ the angular position, $\theta_2(t)$, of Link 2,

$x_8(t) =$ the angular velocity, $\dot{\theta}_1(t)$, of Link 1,

$x_9(t) =$ the angular velocity, $\dot{\theta}_2(t)$, of Link 2,

$u_3(t) =$ the angular acceleration, $\ddot{\theta}_1(t)$, of Link 1,

$u_4(t) =$ the angular acceleration, $\ddot{\theta}_2(t)$, of Link 2.

For the platform, let:

$x_3(t) =$ the angular position, $\theta_0(t)$, of platform,

$x_6(t) =$ the linear velocity of the wheels,

$x_7(t) =$ the angular velocity, $\dot{\theta}_0(t)$, of platform,

$u_1(t) =$ the linear acceleration of the wheels

$u_2(t) =$ the angular acceleration, $\ddot{\theta}_0(t)$, of platform,

Then, at time t and using equation (6.6), we have (on suppressing t),

$$\left.\begin{aligned}
\dot{x}_1 &= x_6 \cos x_3 - l x_7 \sin x_3 - x_7 l_1 \sin(x_3 + x_4) \\
&\quad -x_8 l_1 \sin(x_3 + x_4) - x_7 l_2 \sin(x_3 + x_4 + x_5) \\
&\quad -x_8 l_2 \sin(x_3 + x_4 + x_5) - x_9 l_2 \sin(x_3 + x_4 + x_5)\,, \\
\dot{x}_2 &= x_6 \sin x_3 + l x_7 \cos x_3 + x_7 l_1 \cos(x_3 + x_4) \\
&\quad +x_8 l_1 \cos(x_3 + x_4) + x_7 l_2 \cos(x_3 + x_4 + x_5) \\
&\quad +x_8 l_2 \cos(x_3 + x_4 + x_5) + x_9 l_2 \cos(x_3 + x_4 + x_5)\,, \\
\dot{x}_3 &= x_7\,, \qquad \dot{x}_6 = u_1\,, \qquad \dot{x}_9 = u_4\,. \\
\dot{x}_4 &= x_8\,, \qquad \dot{x}_7 = u_2\,, \\
\dot{x}_5 &= x_9\,, \qquad \dot{x}_8 = u_3\,.
\end{aligned}\right\} \tag{6.7}$$

We shall use the vector $\mathbf{x} = (x_1, ..., x_9)$ to describe the variables in system (6.7). Also, we define the vector $\mathbf{e} = p_1, p_2, p_3, p_4, p_5, 0, 0, 0, 0)$. Here, we define (p_1, p_2) as the final configuration of the End-effector at the target, p_3 as the angular position of the platform at the target and p_4, p_5 as the angular positions of the arm at the target.

6.4 Avoidance Functions

6.4.1 Avoidance of Singular Configurations.

The singular configurations occur when $\theta_2 = x_5 = 0, \pi$ in the anticlockwise direction or $\theta_2 = x_5 = -\pi$ in the clockwise direction. For the configuration, consider the functions

$$W_1(\mathbf{x}) = |x_5|$$

and

$$W_2(\mathbf{x}) = \pi - |x_5|,$$

for $x_5 \in (-\pi, 0) \cup (0, \pi)$.

6.5 Target Attraction and Obstacle Avoidance

The Lyapunov function of our system must be exactly zero at the target center. Consequently we introduce:

$$F_1(\mathbf{x}) = \frac{1}{2}\left[(x_1 - p_1)^2 + (x_2 - p_2)^2\right] \geq 0$$

6.5.1 A Lyapunov Function

Here, we consider a tentative Lyapunov function and the controllers. For constants $\beta_i > 0$, $i = 1, ..., 2$, we consider

$$V(\mathbf{x}) = V_1(\mathbf{x}) + F_1(\mathbf{x}) \sum_{i=1}^{2} \frac{\beta_i}{W_i(\mathbf{x})}$$

on the domain

$$\mathbb{D}(V) = \{\mathbf{x} \ \in \ \mathbf{R}^{10} : W_i > 0, i = 1, 2\}$$

where β_i is a positive constant, W_i are mentioned in Subsection 6.4.1 and

$$V_1(\mathbf{x}) = \frac{1}{2}\,[(x_1 - p_1)^2 + (x_2 - p_2)^2 + x_6^2 + x_7^2 + x_8^2 + x_9^2].$$

Then along a particular trajectory of system (6.7) in $\mathbb{D}(V)$, we have, for $\alpha_1 > 0$, $\alpha_2 > 0$, $\alpha_3 > 0$ and $\alpha_4 > 0$, the time-derivative

$$\begin{aligned} \dot{V}(\mathbf{x}) &= \dot{V}_1(\mathbf{x}) + \dot{F}_1(\mathbf{x}) \sum_{i=1}^{2} \frac{\beta_i}{W_i} - F_1(\mathbf{x}) \sum_{i=1}^{2} \frac{\beta_i \dot{W}_i}{W_i^2} \\ &= \{G_1(\mathbf{x}) + u_1\}x_6 + \{G_2(\mathbf{x}) + u_2\}x_7 + \{G_3(\mathbf{x}) + u_3\}x_8 + \{G_4(\mathbf{x}) + u_4\}x_9 \\ &= -\alpha_1 x_6^2 - \alpha_2 x_7^2 - \alpha_3 x_8^2 - \alpha_4 x_9^2 \leq 0, \end{aligned}$$

if we let $u_1 = -\alpha_1 x_6 - G_1$, $u_2 = -\alpha_2 x_7 - G_2$, $u_3 = -\alpha_3 x_8 - G_3$ and $-\alpha_4 x_9 = G_4 + u_4$ as the *nonlinear controllers*, where G_1, G_2, G_3 and G_4 are defined in Appendix A.6. Also, we see that for $\mathbf{e} = (p_1, p_2, p_3, p_4, p_5, 0, 0, 0, 0)$, we have $V(\mathbf{e}) = \mathbf{0}$, and since $\mathbf{e} \in \mathbb{D}(V)$, we may take $\mathbb{D}(V)$ as the neighbourhood $\mathbb{D}$ of the point $\mathbf{e} = (p_1, p_2, p_3, p_4, p_5, 0, 0, 0, 0)$. Since $\dot{V}(\mathbf{x})$ is nonpositive and continuous for all $\mathbf{x} \in \mathbb{D}(V)$, by Lyapunov's stability Theorem 1.5.1, V is a Lyapunov function for system (6.7) on $\mathbb{D}(V)$ establishing the stability of $\mathbf{e}$. Hence, $\mathbf{e}$ is an equilibrium point of system (6.7), and our Lyapunov function satisfies Theorem 1.5.1 at this equilibrium point.

Thus, we have the system

$$\left.\begin{aligned}
\dot{x}_1 &= x_6\cos x_3 - lx_7\sin x_3 - x_7l_1\sin(x_3+x_4)\\
&\quad -x_8l_1\sin(x_3+x_4) - x_7l_2\sin(x_3+x_4+x_5)\\
&\quad -x_8l_2\sin(x_3+x_4+x_5) - x_9l_2\sin(x_3+x_4+x_5)\,,\\
\dot{x}_2 &= x_6\sin x_3 + lx_7\cos x_3 + x_7l_1\cos(x_3+x_4)\\
&\quad +x_8l_1\cos(x_3+x_4) + x_7l_2\cos(x_3+x_4+x_5)\\
&\quad +x_8l_2\cos(x_3+x_4+x_5) + x_9l_2\cos(x_3+x_4+x_5)\,,\\
\dot{x}_3 &= \tfrac{x_6}{l}\tan(x_3) = x_7\,, \qquad \dot{x}_6 = -\alpha_1x_6 - G_1\,, \qquad \dot{x}_9 = -\alpha_1x_9 - G_4\,,\\
\dot{x}_4 &= x_8\,, \qquad \dot{x}_7 = -\alpha_2x_7 - G_2\,,\\
\dot{x}_5 &= x_9\,, \qquad \dot{x}_8 = -\alpha_3x_8 - G_3\,,
\end{aligned}\right\} \tag{6.8}$$

which is stable at the equilibrium point $\mathbf{e} = (p_1, p_2, p_3, p_4, p_5, 0, 0, 0, 0)$.

6.6 A computer Simulation

The computer is used to numerically integrate system (6.8) to obtain the solution $(x_1, ..., x_8)$ and plot the points $(x_1(t), x_2(t))$ at time t in the x_1x_2-plane until the points converge to a neighbourhood of (p_1, p_2) and stay there as $t \to \infty$. Table 6.1 below gives the parameters, and Figure 6.2 on page 70 gives the trajectory of the arm while Table 6.2 below gives the parameters, and Figure 6.6 on page 72 gives the trajectory of the arm for Scenario 1 example and Scenario 2 example respectively. Notice the slowing down of the car-like mobile manipulator as it approaches its final configuration. This could be explained in terms of the potential energy "cup" of the Lyapunov function derived by Vanualailai and Bibhya [15]. The arm reaches its final configuration in about 10 units of time. In Figure 6.6 on page 72, the first three links are drawn every 0.01 units of time.

Table 6.1: A Scenario 1 example.

Lengths of Links	$l = 3.5, l_1 = 2$ and $l_2 = 2$
Initial Conditions	$\mathbf{x} = (12.63854, 8.793155, \pi/6, \pi/3, -2\pi/3, 15, \pi/180, \pi/180, \pi/180)$
Planar Target	$(p_1, p_2) = (4, 7)$
Control Parameters	$\beta_1 = \beta_2 = 50$
Convergence Parameters	$\alpha_1 = 100, \alpha_2 = 120, \alpha_3 = 170$ and $\alpha_4 = 200$

Table 6.2: A Scenario 2 example.

Lengths of Links	$l = 3.5, l_1 = 2$ and $l_2 = 2$
Initial Conditions	$\mathbf{x} = (\sqrt{3} + 7, 6, \pi/6, \pi/3, -2\pi/3, 550, \pi/180, \pi/180, \pi/180)$
Planar Target	$(p_1, p_2) = (6, 10)$
Control Parameters	$\beta_1 = \beta_2 = 50$
Convergence Parameters	$\alpha_1 = 100, \alpha_2 = 120, \alpha_3 = 170$ and $\alpha_4 = 200$

Figure 6.2 on page 70 and Figure 6.6 on page 72 present snapshots of the motion of the car-like mobile manipulator for Scenario 1 example and Scenario 2 example respectively. The given path for the end-effector (solid line) and the front point of the platform (dashed line) are shown in Figure 6.3 on page 71. In Figure 6.4 on page 71, u_1 (dashed line), u_2 (bold line) and in Figure 6.5 on page 72, u_3 (dashed line) and u_4 (bold line) show the behaviour of the controllers along the trajectory of the car like mobile manipulator. It can be seen that the controllers converge to 0 as time $t{\to}\infty$.

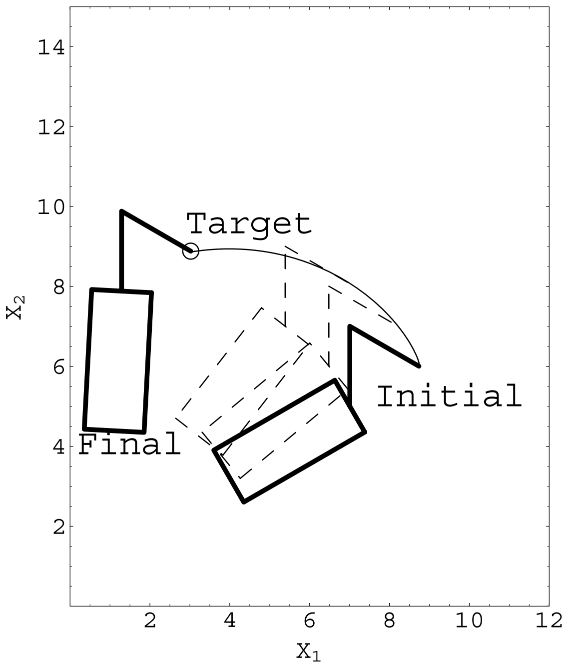

Figure 6.2: Animation of the motion of the car-like mobile manipulator.

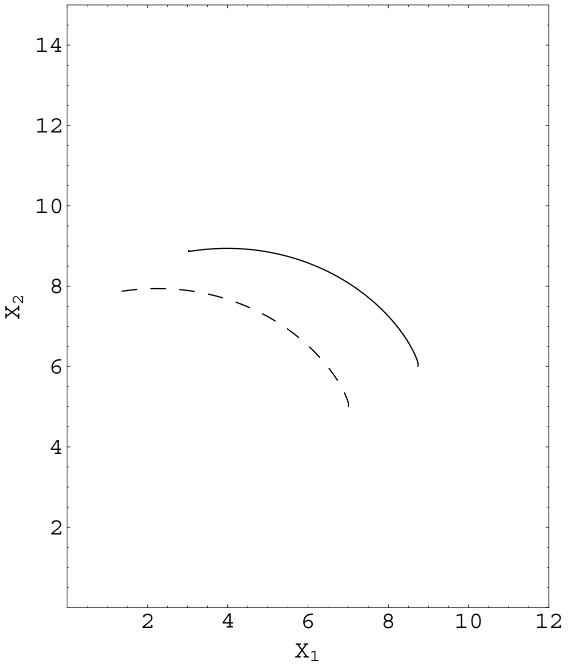

Figure 6.3: Desired platform and end-effector path.

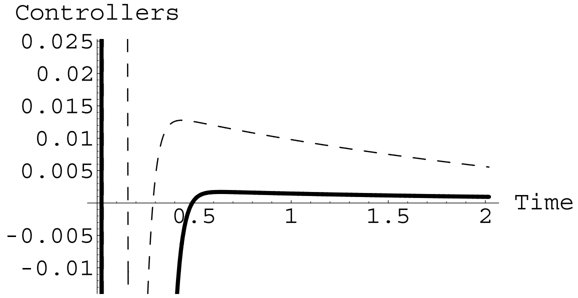

Figure 6.4: Behaviour of the nonlinear controllers; u_1 (dashed line), u_2 (bold line).

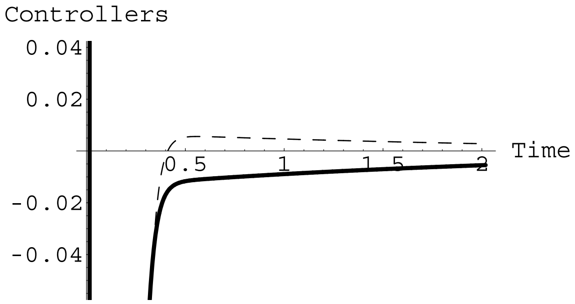

Figure 6.5: Behaviour of the nonlinear controllers; u_3 (dashed line) and u_4 (bold line).

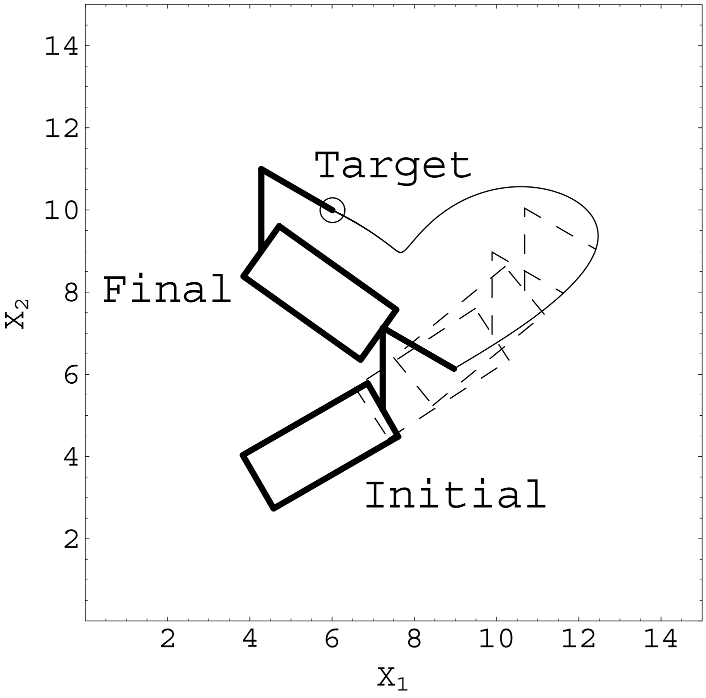

Figure 6.6: Animation of the motion of the car-like mobile manipulator.

6.6.1 Remark

Under the proposed controllers, we saw that the car-like mobile manipulator reached its target safely having a smooth trajectory in both of the scenario examples. The car-like mobile manipulator can be used for transportation tasks, surveillance, automated inspection and cleaning. It can also be used in bush fire fighting where many vehicles (agents) co-operate to fight the fire. Here, they need to decide in following the shortest path and the direction such that they reach the fire quickly.

Chapter 7

Conclusion

In Chapters 2 and 3 we have reviewed the work done by Vaualailai and Sharma [15] and successfully applied Lyapunov's second method to extract the analytical laws that control the 3-link anchored manipulator in a rectangle to its target safely while avoiding collision with the fixed/mobile obstacles. The simulations verify the methodology.

In Chapter 4, we have presented new controllers for motion planning of dual-arm cooperative manipulators. The results obtained illustrated the effectiveness of the controllers.

In Chapters 5 and 6, we have reviewed the work done by Papadopoulos and Poulakakis [13], Seraji [14], Yamamoto and Yun [16] and successfully applied Lyapunov's second to extract the navigational laws that control the motion of the differential-drive and car-like drive mobile manipulators. The controllers yielded admissible input trajectories that drove both the manipulator and the platform to a final configuration. The resulting paths and trajectories are smooth and it has been verified in the simulations.

Clearly, a Lyapunov function which ensures asymptotic stability is more desirable. This is the most challenging part of the Lyapunov method, given the difficulty in constructing such a function for the findpath problem. A new development in this direction is to guarantee stability and also prove that certain sets of initial conditions ensure asymptotic stability.

In this thesis, to simplify discussions, we had considered a stable equilibrium point and then used a computer to decide which system parameters to use for a desirable run. These parameters were $\beta_i^{'}s$, which can be called *control parameters*, and α_1 and α_2, which can be called *convergence parameters*. It had been shown that the larger a control parameter is, the greater is the repulsion from the associated abstacle, and the larger a convergence parameter is, the slower is the trajectory [15].

Research in efficient motion planning for general nonholonomic systems can proceed in many ways. New approaches using metric or other properties of nonholonomic distributions might lead to path planners which work for more general classes of systems. Computational approaches might also be extended to handle higher dimensional systems with very few structural requirements.

A possible approach to control of nonholonomic systems is the study of controllability along a reference trajectory. If we are given a desired state trajectory, we would like to construct a controller which stabilizes the system to this trajectory. Although the existence of a trajectory is guaranteed by the appropriate controllability conditions, construction of a trajectory for systems with drift is still a challenging problem.

In conclusion, as robots take over more things in our lives the interest in theory of robot motion planning and computational complexity results is expected to subside whereas the interest in approximation algorithms and applications will grow more and more.

Bibliography

[1] Barraquand, J. and J. C. Latombe [1989], On nonholonnomic mobile robots and optimal maneuvering, *Proc. of 4th IEEE Int. Symp. on Intelligent Control*, 340-347.

[2] Carriker, W. F., P. K. Khosla, and B. H. Krogh [1990], The use of simulated annealing to solve the mobile manipulator path planning problem, *Proc. of IEEE Int. Conf. on Robotics and Automation*, 204-209.

[3] Deo, A. [2001], *Nonlinear Controllers for a planar vehicle*, MSc thesis, The University of the South Pacific, Fiji.

[4] Ha, J. and J. Vanualailai [1998], A collision avoidance control problem for moving objects and a robot arm, *Journal of Korean Mathematical Society*, **35**, 135-148.

[5] Hootsmans, N. A. M. and S. Dubowsky [1991], Large motion control of mobile manipulators including vehicle suspension characteristics, *Proc. of IEEE Int. Conf. on Robotics and Automation*, 2336-2341.

[6] Kantabutra, V. [1997], Reaching a point with an Aanchored robot arm in a square, *International Journal of Computational Geometry and Applications*, **7**, 539-549.

[7] Krevald, M. V., J. Snoeyink, and S. H. Whitesides [1996], Folding rulers inside triangles, *Discrete and Computational Geometry*, **15**, 265-285.

[8] Liu, K. and F. L. Lewis [1992], Control of mobile robot with onboard manipulator, *Proc. of Int. Symp. on Robotics and Manufacturing*, **4**, 539-546.

[9] Lyapunov, A. M. [1892], The general problem of the stability of motion, *International Journal of Control : Lyapunov's Century Issue*, **55**, No.3.

[10] Meyer, W. [1993], Moving a planar robot arm, *MAA Notes Number* **29**, *The Mathematical Association of America*, 180-192.

[11] Miksch, W. and D. S. Schroeder [1992], Performance-functional based controller design for a mobile manipulator, *Proc. of IEEE Int. Conf. on Robotics and Automation*, **1**, 227-232.

[12] Murray, R. M. and S. S. Sastry [1993], Nonholonomic motion planning: steering using sinusoids, *IEEE Trans. on Automatic Control*, **38**, 700-716.

[13] Papadopoulos, E. and J. Poulakakis [2000], Trajectory planning and control for mobile manipulator systems, *Proc. of 8th IEEE Medit. Conf. on Control and Automation*, Patras, Greek.

[14] Seraji, H. [1998], A unified approach to motion control of motion control of mobile manipulators, *International Journal of Robotics Research*, **17**, 107-118.

[15] Vanualailai, J. and B. N. Sharma [2003], Moving a robot arm: an interesting Application of the Direct method of Lyapunov, *Southwest Journal of Pure and Applied Mathematics*, issue 1, 43-45.

[16] Yamamoto, Y. and X. Yun [1994], Coordinating locomotion and manipulation of a mobile manipulator, *IEEE Trans. Autom. Control*, **39**, 1326-1332.

Appendix A

A.1 Derivatives of components in Subsection 2.4.1

The separate components of $\dot{V}(\mathbf{x})$ are :

$$
\begin{aligned}
\dot{V}_0(\mathbf{x}) &= (x_1 - p_1)\dot{x_1} + (x_2 - p_2)\dot{x_2} + x_6\dot{x_6} + x_7\dot{x_7} + x_8\dot{x_8} \\
&= (x_1 - p_1)[-x_6x_2 - x_7(x_2 - l_1 \sin x_3) - x_8(x_2 - l_1 \sin x_3 - l_2 \sin(x_3 + x_4))] \\
&\quad + (x_2 - p_2)[x_6x_1 + x_7(x_1 - l_1 \cos x_3) + x_8(x_1 - l_1 \cos x_3 - l_2 \cos(x_3 + x_4))] \\
&\quad + x_6u_1 + x_7u_2 + x_8u_3
\end{aligned}
$$

$$
\begin{aligned}
\dot{F}_0(\mathbf{x}) \sum_{i=1}^{17} \frac{\beta_i}{W_i} &= ((x_1 - p_1) - x_6x_2 - x_7(x_2 - l_1 \sin x_3) - x_8[x_2 - l_1 \sin x_3 - l_2 \sin(x_3 + x_4)] \\
&\quad + (x_2 - p_2)x_6x_1 + x_7(x_1 - l_1 \cos x_3) + x_8[x_1 - l_1 \cos x_3 - l_2 \cos(x_3 + x_4)]) \\
&\quad \left(\sum_{i=1}^{17} \frac{\beta_i}{W_i} \right)
\end{aligned}
$$

$$\begin{aligned}
-F_0(\mathbf{x})\sum_{i=1}^{17}\frac{\beta_i\dot{W}_i}{{W_i}^2} \quad = \quad & -\left[\frac{F_0\beta_1 x_4}{W_1^2|x_4|}-\frac{F_0\beta_2 x_4}{W_2^2|x_4|}\right]x_7-\left[\frac{F_0\beta_3 x_5}{W_3^2|x_5|}-\frac{F_0\beta_4 x_5}{W_4^2|x_5|}\right]x_8 \\
& -\frac{F_0\beta_5}{W_5^2}[-x_6x_2-x_7(x_2-l_1\sin x_3)-x_8(x_2-l_1\sin x_3-l_2\sin(x_3+x_4))] \\
& +\frac{F_0\beta_6}{W_6^2}[-x_6x_2-x_7(x_2-l_1\sin x_3)-x_8(x_2-l_1\sin x_3-l_2\sin(x_3+x_4))] \\
& -\frac{F_0\beta_7}{W_7^2}[x_6x_1+x_7(x_1-l_1\cos x_3)+x_8(x_1-l_1\cos x_3-l_2\cos(x_3+x_4))] \\
& +\frac{F_0\beta_8}{W_8^2}[x_6x_1+x_7(x_1-l_1\cos x_3)+x_8(x_1-l_1\cos x_3-l_2\cos(x_3+x_4))] \\
& -\frac{F_0\beta_9 x_6}{W_9^2}+\frac{F_0\beta_{10}x_6}{W_{10}^2}+\frac{F_0\beta_{11}l_1x_6\cos x_3}{W_{11}^2}-\frac{F_0\beta_{12}l_1x_6\sin x_3}{W_{12}^2} \\
& +\frac{F_0\beta_{13}l_1x_6\cos x_3}{W_{13}^2}+\frac{F_0\beta_{13}l_2\cos(x_3+x_4)x_6}{W_{13}^2}+\frac{F_0\beta_{13}l_2\cos(x_3+x_4)x_7}{W_{13}^2} \\
& -\frac{F_0\beta_{14}l_1x_6\sin x_3}{W_{14}^2}-\frac{F_0\beta_{14}l_1\sin(x_3+x_4)x_6}{W_{14}^2}-\frac{F_0\beta_{14}l_2\sin(x_3+x_4)x_7}{W_{14}^2} \\
& -\frac{F_0\beta_{15}l_1x_6\cos x_3}{W_{15}^2}-\frac{F_0\beta_{15}l_2\cos(x_3+x_4)x_6l_2\sin(x_3+x_4)}{W_{15}^2|l_2\sin(x_3+x_4)|} \\
& -\frac{F_0\beta_{15}l_2\cos(x_3+x_4)x_7l_2\sin(x_3+x_4)}{W_{15}^2|l_2\sin(x_3+x_4)|} \\
& +\frac{F_0\beta_{16}l_1x_6\sin x_3}{W_{16}^2}+\frac{F\beta_{16}l_2\sin(x_3+x_4)x_6l_2\cos(x_3+x_4)}{W_{16}^2|l_2\cos(x_3+x_4)|} \\
& +\frac{F_0\beta_{16}l_2\sin(x_3+x_4)x_7l_2\cos(x_3+x_4)}{W_{16}^2|l_2\cos(x_3+x_4)|} \\
& -\frac{F_0\beta_{17}}{W_{17}^2}(x_1-o_1)[-x_6x_2-x_7(x_2-l_1\sin x_3)] \\
& -\frac{F_0\beta_{17}}{W_{17}^2}(x_1-o_1)[-x_8(x_2-l_1\sin x_3-l_2\sin(x_3+x_4))] \\
& -\frac{F_0\beta_{17}}{W_{17}^2}(x_2-o_2)[x_6x_1+x_7(x_1-l_1\cos x_3)] \\
& -\frac{F_0\beta_{17}}{W_{17}^2}(x_2-o_2)[x_8(x_1-l_1\cos x_3-l_2\cos(x_3+x_4))]
\end{aligned}$$

$$
\begin{aligned}
\dot{V}(\mathbf{x}) \;=\;& \{[(x_2-p_2)x_1-(x_1-p_1)x_2]\left(1+\sum_{i=1}^{17}\frac{\beta_i}{W_i}\right)+u_1\\
&+F_0\{x_2\left(\frac{\beta_5}{W_5^2}-\frac{\beta_6}{W_6^2}\right)+x_1(\frac{\beta_8}{W_8^2}-\frac{\beta_7}{W_7^2})\\
&+\frac{\beta_{10}}{W_{10}^2}-\frac{\beta_9}{W_9^2}+l_1\cos x_3\left(\frac{\beta_{11}}{W_{11}^2}+\frac{\beta_{13}}{W_{13}^2}\right)-l_1\sin x_3\left(\frac{\beta_{12}}{W_{12}^2}+\frac{\beta_{14}}{W_{14}^2}\right)\\
&+l_2\left[\frac{\beta_{13}\cos(x_3+x_4)}{W_{13}^2}-\frac{\beta_{14}\sin(x_3+x_4)}{W_{14}^2}\right]\\
&-\frac{l_1\beta_{15}\cos x_3}{W_{15}^2}-\frac{\beta_{15}l_2^2\cos(x_3+x_4)\sin(x_3+x_4)}{W_{15}^2|l_2\sin(x_3+x_4)|}\\
&+\frac{l_1\beta_{16}\sin x_3}{W_{16}^2}+\frac{\beta_{16}l_2^2\cos(x_3+x_4)\sin(x_3+x_4)}{W_{16}^2|l_2\cos(x_3+x_4)|}\\
&+\frac{\beta_{17}^2}{W_{17}^2}[(x_1-o_1)x_2-(x_2-o_2)x_1]\}\}x_6\\
&+\{[(x_2-p_2)(x_1-l_1\cos x_3)-(x_1-p_1)(x_2-l_1\sin x_3)]\left(1+\sum_{i=1}^{17}\frac{\beta_i}{W_i}\right)+u_2\\
&+F_0\{\left(\frac{\beta_2}{W_2^2}-\frac{\beta_1}{W_1^2}\right)\frac{x_4}{|x_4|}+(x_2-l_1\sin x_3)\left(\frac{\beta_5}{W_5^2}-\frac{\beta_6}{W_6^2}\right)\\
&+(x_1-l_1\cos x_3)\left(\frac{\beta_8}{W_8^2}-\frac{\beta_7}{W_7^2}\right)\\
&+l_2\left[\frac{\beta_{13}\cos(x_3+x_4)}{W_{13}^2}-\frac{\beta_{14}\sin(x_3+x_4)}{W_{14}^2}\right]\\
&+l_2\sin(x_3+x_4)\cos(x_3+x_4)\left[\frac{\beta_{16}}{W_{16}^2|l_2\cos(x_3+x_4)|}-\frac{\beta_{15}}{W_{15}^2|l_2\sin(x_3+x_4)|}\right]\\
&+\frac{\beta_{17}}{W_{17}^2}[(x_2-l_1\sin x_3)(x_1-o_1)-(x_1-l_1\cos x_3)(x_2-o_2)]\}\}x_7\\
&+\{[(x_2-p_2)(x_1-l_1\cos x_3-l_2\cos(x_3+x_4))]\left(1+\sum_{i=1}^{17}\frac{\beta_i}{W_i}\right)\\
&-[(x_1-p_1)(x_2-l_1\sin x_3-l_2\sin(x_3+x_4))]\left(1+\sum_{i=1}^{17}\frac{\beta_i}{W_i}\right)\\
&+u_3+F_0\{\left(\frac{\beta_4}{W_4^2}-\frac{\beta_3}{W_3^2}\right)\frac{x_5}{|x_5|}+[(x_2-p_2)(x_2-l_1\sin x_3-l_2\sin(x_3+x_4))]\\
&\left(\frac{\beta_5}{W_5^2}-\frac{\beta_6}{W_6^2}\right)+(x_1-l_1\cos x_3-l_2\cos(x_3+x_4))\left(\frac{\beta_8}{W_8^2}-\frac{\beta_7}{W_7^2}\right)
\end{aligned}
$$

$$
\begin{aligned}
&+ \frac{\beta_{17}}{W_{17}^2}[(x_2 - l_1 \sin x_3 - l_2 \sin(x_3 + x_4))(x_1 - o_1) \\
&- (x_1 - l_1 \cos x_3 - l_2 \cos(x_3 + x_4))(x_2 - o_2)]\}\}x_8 \\
= \;& \{G_1(\mathbf{x}) + u_1\}x_6 + \{G_2(\mathbf{x}) + u_2\}x_7 + \{G_3(\mathbf{x}) + u_3\}x_8 \\
= \;& \{G_1 + u_1\}x_6 + \{G_2 + u_2\}x_7 + \{G_3 + u_3\}x_8
\end{aligned}
$$

A.2 Derivatives of components in Subsection 2.6.1

The separate components of $\dot{V}(\mathbf{x})$ are :

$$
\begin{aligned}
\dot{V}_1(\mathbf{x}) &= \frac{(x_2 - p_2)}{|x_2 - p_2|}\dot{x_2} + \frac{x_6}{|x_6|}\dot{x_6} + \frac{x_7}{|x_7|}\dot{x_7} + \frac{x_8}{|x_8|}\dot{x_8} \\
&= \frac{(x_2 - p_2)}{|x_2 - p_2|}[x_6 x_1 + x_7(x_1 - l_1 \cos x_3) + x_8(x_1 - l_1 \cos x_3 - l_2 \cos(x_3 + x_4))] \\
&\quad + \frac{x_6}{|x_6|}u_1 + \frac{x_7}{|x_7|}u_2 + \frac{x_8}{|x_8|}u_3
\end{aligned}
$$

$$
\begin{aligned}
\dot{F_1}(\mathbf{x}) \sum_{i=1}^{5} \frac{\beta_i}{W_i} &= \left\{ \frac{(x_2 - p_2)}{|x_2 - p_2|}[x_6 x_1 + x_7(x_1 - l_1 \cos x_3) + x_8(x_1 - l_1 \cos x_3 - l_2 \cos(x_3 + x_4))] \right\} \\
&\quad \left(\sum_{i=1}^{5} \frac{\beta_i}{W_i} \right)
\end{aligned}
$$

$$
\begin{aligned}
-F_1(\mathbf{x}) \sum_{i=1}^{5} \frac{\beta_i \dot{W}_i}{{W_i}^2} &= \left[\frac{F_1 \beta_5 x_2}{W_5^2} \right] x_6 - \left[\frac{F_1 \beta_1 x_4}{W_1^2 |x_4|} - \frac{F_1 \beta_2 x_4}{W_2^2 |x_4|} - \frac{F_1 \beta_5 (x_2 - l_1 \sin x_3)}{W_5^2} \right] x_7 \\
&\quad - \left[\frac{F_1 \beta_3 x_5}{W_3^2 |x_5|} - \frac{F_1 \beta_4 x_5}{W_4^2 |x_5|} - \frac{F_1 \beta_5 (x_2 - l_1 \sin x_3 - l_2 \sin(x_3 + x_4))}{W_5^2} \right] x_8
\end{aligned}
$$

$$
\begin{aligned}
\dot{V}(\mathbf{x}) &= \Bigg\{\left[\frac{(x_2-p_2)}{|x_2-p_2|}x_1\right]\left(1+\sum_{i=1}^{5}\frac{\beta_i}{W_i}\right)+\frac{u_1}{|x_6|}+\frac{F_1\beta_5x_2}{W_5^2}\Bigg\}x_6\\
&\quad+\{\left[\frac{(x_2-p_2)}{|x_2-p_2|}(x_1-l_1\cos x_3)\right]\left(1+\sum_{i=1}^{5}\frac{\beta_i}{W_i}\right)+\frac{u_2}{|x_7|}\\
&\quad+F_1\left[\left(\frac{\beta_2}{W_2^2}-\frac{\beta_1}{W_1^2}\right)\frac{x_4}{|x_4|}+\frac{\beta_5(x_2-l_1\sin x_3)}{W_5^2}\right]\}x_7\\
&\quad+\{\left[\frac{(x_2-p_2)}{|x_2-p_2|}(x_1-l_1\cos x_3-l_2\cos(x_3+x_4))\right]\left(1+\sum_{i=1}^{5}\frac{\beta_i}{W_i}\right)\\
&\quad+\frac{u_3}{|x_8|}+F_1\Bigg\{\left(\frac{\beta_4}{W_4^2}-\frac{\beta_3}{W_3^2}\right)\frac{x_5}{|x_5|}+\frac{\beta_5(x_2-l_1\sin x_3-l_2\sin(x_3+x_4))}{W_5^2}\Bigg\}\}x_8\\
&= \left\{G_4(\mathbf{x})+\frac{u_1}{|x_6|}\right\}x_6+\left\{G_5(\mathbf{x})+\frac{u_2}{|x_7|}\right\}x_7+\left\{G_6(\mathbf{x})+\frac{u_3}{|x_8|}\right\}x_8\\
&= \left\{G_4+\frac{u_1}{|x_6|}\right\}x_6+\left\{G_5+\frac{u_2}{|x_7|}\right\}x_7+\left\{G_6+\frac{u_3}{|x_8|}\right\}x_8
\end{aligned}
$$

A.3 Derivatives of components in Subsection 3.4.1

The separate components of $\dot{V}(\mathbf{x})$ are :

$$
\begin{aligned}
\dot{V_2}(\mathbf{x}) &= (x_1-p_1)\dot{x_1}+(x_2-p_2)\dot{x_2}+x_6\dot{x_6}+x_7\dot{x_7}+x_8\dot{x_8}\\
&= (x_1-p_1)[-x_6x_2-x_7(x_2-l_1\sin x_3)-x_8(x_2-l_1\sin x_3-l_2\sin(x_3+x_4))]\\
&\quad+(x_2-p_2)[x_6x_1+x_7(x_1-l_1\cos x_3)+x_8(x_1-l_1\cos x_3-l_2\cos(x_3+x_4))]\\
&\quad+x_6u_1+x_7u_2+x_8u_3+(x_9-p_3)x_{11}+(x_{10}-p_4)x_{12}+x_{11}u_4+x_{12}u_5
\end{aligned}
$$

$$
\begin{aligned}
\dot{F_2}(\mathbf{x})\sum_{i=1}^{17}\frac{\beta_i}{W_i} &= \{(x_1-p_1)[-x_6x_2-x_7(x_2-l_1\sin x_3)-x_8(x_2-l_1\sin x_3-l_2\sin(x_3+x_4))]\\
&\quad+(x_2-p_2)[x_6x_1+x_7(x_1-l_1\cos x_3)+x_8(x_1-l_1\cos x_3-l_2\cos(x_3+x_4))]\\
&\quad+(x_9-p_3)x_{11}+(x_{10}-p_4)x_{12}\}\left(\sum_{i=1}^{17}\frac{\beta_i}{W_i}\right)
\end{aligned}
$$

$$
\begin{aligned}
-F_2(\mathbf{x})\sum_{i=1}^{17}\frac{\beta_i\dot{W}_i}{W_i{}^2} \quad = \quad & -\left[\frac{F_2\beta_1x_4}{W_1^2|x_4|}-\frac{F_2\beta_2x_4}{W_2^2|x_4|}\right]x_7-\left[\frac{F_2\beta_3x_5}{W_3^2|x_5|}-\frac{F_2\beta_4x_5}{W_4^2|x_5|}\right]x_8 \\
& -\frac{F_2\beta_5}{W_5^2}[-x_6x_2-x_7(x_2-l_1\sin x_3)-x_8(x_2-l_1\sin x_3-l_2\sin(x_3+x_4))] \\
& +\frac{F_2\beta_6}{W_6^2}[-x_6x_2-x_7(x_2-l_1\sin x_3)-x_8(x_2-l_1\sin x_3-l_2\sin(x_3+x_4))] \\
& -\frac{F_2\beta_7}{W_7^2}[x_6x_1+x_7(x_1-l_1\cos x_3)+x_8(x_1-l_1\cos x_3-l_2\cos(x_3+x_4))] \\
& +\frac{F_2\beta_8}{W_8^2}[x_6x_1+x_7(x_1-l_1\cos x_3)+x_8(x_1-l_1\cos x_3-l_2\cos(x_3+x_4))] \\
& -\frac{F_2\beta_9x_6}{W_9^2}+\frac{F_2\beta_{10}x_6}{W_{10}^2}+\frac{F_2\beta_{11}l_1x_6\cos x_3}{W_{11}^2}-\frac{F_2\beta_{12}l_1x_6\sin x_3}{W_{12}^2} \\
& +\frac{F_2\beta_{13}l_1x_6\cos x_3}{W_{13}^2}+\frac{F_2\beta_{13}l_2\cos(x_3+x_4)x_6}{W_{13}^2}+\frac{F\beta_{13}l_2\cos(x_3+x_4)x_7}{W_{13}^2} \\
& -\frac{F_2\beta_{14}l_1x_6\sin x_3}{W_{14}^2}-\frac{F_2\beta_{14}l_1\sin(x_3+x_4)x_6}{W_{14}^2}-\frac{F_2\beta_{14}l_2\sin(x_3+x_4)x_7}{W_{14}^2} \\
& -\frac{F_2\beta_{15}l_1x_6\cos x_3}{W_{15}^2}-\frac{F\beta_{15}l_2\cos(x_3+x_4)x_6l_2\sin(x_3+x_4)}{W_{15}^2|l_2\sin(x_3+x_4)|} \\
& -\frac{F_2\beta_{15}l_2\cos(x_3+x_4)x_7l_2\sin(x_3+x_4)}{W_{15}^2|l_2\sin(x_3+x_4)|} \\
& +\frac{F_2\beta_{16}l_1x_6\sin x_3}{W_{16}^2}+\frac{F\beta_{16}l_2\sin(x_3+x_4)x_6l_2\cos(x_3+x_4)}{W_{16}^2|l_2\cos(x_3+x_4)|} \\
& +\frac{F\beta_{16}l_2\sin(x_3+x_4)x_7l_2\cos(x_3+x_4)}{W_{16}^2|l_2\cos(x_3+x_4)|} \\
& -\frac{F_2\beta_{17}}{W_{17}^2}(x_1-x_9)[-x_6x_2-x_7(x_2-l_1\sin x_3)] \\
& -\frac{F_2\beta_{17}}{W_{17}^2}(x_1-x_9)[-x_8(x_2-l_1\sin x_3-l_2\sin(x_3+x_4))] \\
& -\frac{F_2\beta_{17}}{W_{17}^2}(x_2-x_{10})[x_6x_1+x_7(x_1-l_1\cos x_3)] \\
& -\frac{F_2\beta_{17}}{W_{17}^2}(x_2-x_{10})[x_8(x_1-l_1\cos x_3-l_2\cos(x_3+x_4))] \\
& +\frac{F_2\beta_{17}}{W_{17}^2}(x_1-x_9)x_{11}+\frac{F_2\beta_{17}}{W_{17}^2}(x_2-x_{10})x_{12}
\end{aligned}
$$

$$
\begin{aligned}
\dot{V}(\mathbf{x}) \;=\;& \{[(x_2-p_2)x_1-(x_1-p_1)x_2]\left(1+\sum_{i=1}^{17}\frac{\beta_i}{W_i}\right)+u_1+F_2\{x_2\left(\frac{\beta_5}{W_5^2}-\frac{\beta_6}{W_6^2}\right)\\
&+x_1\left(\frac{\beta_8}{W_8^2}-\frac{\beta_7}{W_7^2}\right)+\frac{\beta_{10}}{W_{10}^2}-\frac{\beta_9}{W_9^2}+l_1\cos(x_3)\left(\frac{\beta_{11}}{W_{11}^2}+\frac{\beta_{13}}{W_{13}^2}\right)\\
&-l_1\sin x_3\left(\frac{\beta_{12}}{W_{12}^2}+\frac{\beta_{14}}{W_{14}^2}\right)\\
&+l_2\left[\frac{\beta_{13}\cos(x_3+x_4)}{W_{13}^2}-\frac{\beta_{14}\sin(x_3+x_4)}{W_{14}^2}\right]\\
&-\frac{l_1\beta_{15}\cos x_3}{W_{15}^2}-\frac{\beta_{15}l_2^2\cos(x_3+x_4)\sin(x_3+x_4)}{W_{15}^2|l_2\sin(x_3+x_4)|}\\
&+\frac{l_1\beta_{16}\sin x_3}{W_{16}^2}+\frac{\beta_{16}l_2^2\cos(x_3+x_4)\sin(x_3+x_4)}{W_{16}^2|l_2\cos(x_3+x_4)|}\\
&+\frac{\beta_{17}}{W_{17}^2}[(x_1-x_9)x_2-(x_2-x_{10})x_1]\}\}x_6\\
&+\{[(x_2-p_2)(x_1-l_1\cos x_3)-(x_1-p_1)(x_2-l_1\sin x_3)]\left(1+\sum_{i=1}^{17}\frac{\beta_i}{W_i}\right)+u_2\\
&+F_2\{\left(\frac{\beta_2}{W_2^2}-\frac{\beta_1}{W_1^2}\right)\frac{x_4}{|x_4|}+(x_2-l_1\sin x_3)\left(\frac{\beta_5}{W_5^2}-\frac{\beta_6}{W_6^2}\right)\\
&+(x_1-l_1\cos x_3)\left(\frac{\beta_8}{W_8^2}-\frac{\beta_7}{W_7^2}\right)+l_2\left[\frac{\beta_{13}\cos(x_3+x_4)}{W_{13}^2}-\frac{\beta_{14}\sin(x_3+x_4)}{W_{14}^2}\right]\\
&+l_2\sin(x_3+x_4)\cos(x_3+x_4)\left[\frac{\beta_{16}}{W_{16}^2|l_2\cos(x_3+x_4)|}-\frac{\beta_{15}}{W_{15}^2|l_2\sin(x_3+x_4)|}\right]\\
&+\frac{\beta_{17}}{W_{17}^2}[(x_2-l_1\sin x_3)(x_1-x_9)-(x_1-l_1\cos x_3)(x_2-x_{10})]\}\}x_7\\
&+\{[(x_2-p_2)(x_1-l_1\cos x_3-l_2\cos(x_3+x_4))]\left(1+\sum_{i=1}^{17}\frac{\beta_i}{W_i}\right)\\
&-[(x_1-p_1)(x_2-l_1\sin x_3-l_2\sin(x_3+x_4))]\left(1+\sum_{i=1}^{17}\frac{\beta_i}{W_i}\right)\\
&+u_3+F_2\{\left(\frac{\beta_4}{W_4^2}-\frac{\beta_3}{W_3^2}\right)\frac{x_5}{|x_5|}+[(x_2-p_2)(x_2-l_1\sin x_3-l_2\sin(x_3+x_4))]\\
&\left(\frac{\beta_5}{W_5^2}-\frac{\beta_6}{W_6^2}\right)+(x_1-l_1\cos x_3-l_2\cos(x_3+x_4))\left(\frac{\beta_8}{W_8^2}-\frac{\beta_7}{W_7^2}\right)\\
&+\frac{\beta_{17}}{W_{17}^2}[(x_2-l_1\sin x_3-l_2\sin(x_3+x_4))(x_1-x_9)\\
&-(x_1-l_1\cos x_3-l_2\cos(x_3+x_4))(x_2-x_{10})]\}\}x_8
\end{aligned}
$$

$$
\begin{aligned}
& + \{(x_9 - p_3)\left(1 + \sum_{i=1}^{17} \frac{\beta_i}{W_i}\right) + u_4 + \frac{F_2\beta_{17}}{W_{17}^2}(x_1 - x_9)\}x_{11} \\
& + \{(x_{10} - p_4)\left(1 + \sum_{i=1}^{17} \frac{\beta_i}{W_i}\right) + u_5 + \frac{F_2\beta_{17}}{W_{17}^2}(x_2 - x_{10})\}x_{12} \\
= \;& \{G_1(\mathbf{x}) + u_1\}x_6 + \{G_2(\mathbf{x}) + u_2\}x_7 + \{G_3(\mathbf{x}) + u_3\}x_8 \\
& + \{G_4(\mathbf{x}) + u_4\}x_{11} + \{G_5(\mathbf{x}) + u_5\}x_{12} \\
= \;& \{G_1 + u_1\}x_6 + \{G_2 + u_2\}x_7 + \{G_3 + u_3\}x_8 + \{G_4 + u_4\}x_{11} + \{G_5 + u_5\}x_{12}
\end{aligned}
$$

A.4 Derivatives of components in Subsection 4.5.3

The separate components of $\dot{V}(x)$ are :

$$
\begin{aligned}
\dot{V_0} = \;& (x_1 - p_1)\dot{x_1} + (x_2 - p_2)\dot{x_2} + (x_1 + l - p_3)\dot{x_1} \\
& + x_{11}\dot{x_{11}} + x_{12}\dot{x_{12}} + x_{13}\dot{x_{13}} + x_{14}\dot{x_{14}} + x_{15}\dot{x_{15}} + x_{16}\dot{x_{16}} \\
= \;& (x_1 - p_1)[-x_{11}x_2 - x_{12}(x_2 - l_1 \sin x_5) - x_{13}l_3 \sin(x_5 + x_6 + x_7)] \\
& + (x_2 - p_2)[x_{11}x_1 + x_{12}(x_1 - l_1 \cos x_5) + x_{13}l_3 \cos(x_5 + x_6 + x_7)] \\
& + (x_1 + l - p_3)[-x_{11}x_2 - x_{12}(x_2 - l_1 \sin x_5) - x_{13}l_3 \sin(x_5 + x_6 + x_7)] \\
& + x_{11}u_1 + x_{12}u_2 + x_{13}u_3 + x_{14}u_4 + x_{15}u_5 + x_{16}u_6
\end{aligned}
$$

$$
\begin{aligned}
\dot{F_3}(x)\sum_{i=1}^{8} \frac{\beta_i}{W_i} = \;& \{(x_1 - p_1)[-x_{11}x_2 - x_{12}(x_2 - l_1 \sin x_5) - x_{13}l_3 \sin(x_5 + x_6 + x_7)] \\
& + (x_2 - p_2)[x_{11}x_1 + x_{12}(x_1 - l_1 \cos x_5) + x_{13}l_3 \sin(x_5 + x_6 + x_7)] \\
& + (x_1 + l - p_3)[-x_{11}x_2 - x_{12}(x_2 - l_1 \sin x_5) - x_{13}l_3 \sin(x_5 + x_6 + x_7)]\}\left(\sum_{i=1}^{8} \frac{\beta_i}{W_i}\right)
\end{aligned}
$$

$$\begin{aligned} -F_3(x)\sum_{i=1}^{8}\frac{\beta_i\dot{W}_i}{W_i} &= -\left[\frac{F_3\beta_1 x_6}{W_1^2|x_6|}-\frac{F_3\beta_2 x_6}{W_2^2|x_6|}\right]x_{12}-\left[\frac{F_3\beta_3 x_7}{W_3^2|x_7|}-\frac{F_3\beta_4 x_7}{W_4^2|x_7|}\right]x_{13} \\ &\quad -\left[\frac{F_3\beta_5 x_9}{W_5^2|x_9|}-\frac{F_3\beta_6 x_9}{W_6^2|x_9|}\right]x_{15}-\left[\frac{F_3\beta_7 x_{10}}{W_7^2|x_{10}|}-\frac{F_3\beta_8 x_{10}}{W_8^2|x_{10}|}\right]x_{16} \end{aligned}$$

$$\begin{aligned} \dot{V}(x) &= \{[(x_2-p_2)x_1-(x_1-p_1)x_2-(x_1+l-p_3)x_2]\left(1+\sum_{i=1}^{8}\frac{\beta_i}{W_i}\right)+u_1\}x_{11} \\ &\quad +\{[(x_2-p_2)(x_1-l_1\cos x_5)-(x_1-p_1)(x_2-l_1\sin x_5) \\ &\quad -(x_1+l-p_3)(x_2-l_1\sin x_5)]\left(1+\sum_{i=1}^{8}\frac{\beta_i}{W_i}\right) \\ &\quad +u_2-F_3\left(\frac{\beta_1}{W_1^2}-\frac{\beta_2}{W_2^2}\right)\frac{x_6}{|x_6|}\}x_{12} \\ &\quad +\{[(x_2-p_2)l_3\cos(x_5+x_6+x_7)-(x_1-p_1)l_3\sin(x_5+x_6+x_7) \\ &\quad -(x_1+l-p_3)l_3\sin(x_5+x_6+x_7)]\left(1+\sum_{i=1}^{8}\frac{\beta_i}{W_i}\right)+u_3-F_3\left(\frac{\beta_3}{W_3^2}-\frac{\beta_4}{W_4^2}\right)\frac{x_7}{|x_7|}\}x_{13} \\ &\quad +u_4x_{14}+\{u_5-F_3\left(\frac{\beta_5}{W_5^2}-\frac{\beta_6}{W_6^2}\right)\frac{x_9}{|x_9|}\}x_{15} \\ &\quad +\{u_6-F_3\left(\frac{\beta_7}{W_7^2}-\frac{\beta_8}{W_8^2}\right)\frac{x_{10}}{|x_{10}|}\}x_{16} \\ &= \{G_1(x)+u_1\}x_{11}+\{G_2(x)+u_2\}x_{12}+\{G_3(x)+u_3\}x_{13} \\ &\quad +u_4x_{14}+\{G_5(x)+u_5\}x_{15}+\{G_6(x)+u_6\}x_{16} \\ &= \{G_1+u_1\}x_{11}+\{G_2+u_2\}x_{12}+\{G_3+u_3\}x_{13} \\ &\quad +u_4x_{14}+\{G_5+u_5\}x_{15}+\{G_6+u_6\}x_{16} \end{aligned}$$

A.5 Derivatives of components in Subsection 5.5.1

The separate components of $\dot{V}(\mathbf{x})$ are :

$$\begin{aligned}
\dot{V}_0(\mathbf{x}) &= (x_1-p_1)\dot{x}_1+(x_2-p_2)\dot{x}_2+x_6\dot{x}_6+x_7\dot{x}_7+x_8\dot{x}_8+x_9\dot{x}_9+x_{10}\dot{x}_{10} \\
&= (x_1-p_1)[\frac{1}{2}(x_6+x_7)\cos x_3-x_8l_G\sin x_3-x_8l_1\sin(x_3+x_4)-x_9l_1\sin(x_3+x_4) \\
&\quad -x_8l_2\sin(x_3+x_4+x_5)-x_9l_2\sin(x_3+x_4+x_5)-x_{10}l_2\sin(x_3+x_4+x_5)] \\
&\quad +(x_2-p_2)[\frac{1}{2}(x_6+x_7)\sin x_3+x_8l_G\cos x_3+x_8l_1\cos(x_3+x_4)+x_9l_1\cos(x_3+x_4) \\
&\quad +x_8l_2\cos(x_3+x_4+x_5)+x_9l_2\cos(x_3+x_4+x_5)+x_{10}l_2\cos(x_3+x_4+x_5)] \\
&\quad +x_6u_1+x_7u_2+x_8u_3+x_9u_4+x_{10}u_5
\end{aligned}$$

$$\begin{aligned}
\dot{F}_0(\mathbf{x})\sum_{i=1}^{2}\frac{\beta_i}{W_i} &= \{(x_1-p_1)[\frac{1}{2}(x_6+x_7)\cos x_3-x_8l_G\sin x_3-x_8l_1\sin(x_3+x_4) \\
&\quad -x_9l_1\sin(x_3+x_4)-x_8l_2\sin(x_3+x_4+x_5)-x_9l_2\sin(x_3+x_4+x_5) \\
&\quad -x_{10}l_2\sin(x_3+x_4+x_5)]+(x_2-p_2)[\frac{1}{2}(x_6+x_7)\sin x_3+x_8l_G\cos x_3 \\
&\quad +x_8l_1\cos(x_3+x_4)+x_9l_1\cos(x_3+x_4)+x_8l_2\cos(x_3+x_4+x_5) \\
&\quad +x_9l_2\cos(x_3+x_4+x_5)+x_{10}l_2\cos(x_3+x_4+x_5)]\} \\
&\quad \left(\sum_{i=1}^{2}\frac{\beta_i}{W_i}\right)
\end{aligned}$$

$$-F_0(\mathbf{x})\sum_{i=1}^{2}\frac{\beta_i\dot{W}_i}{{W_i}^2} = -\left[\frac{F_0\beta_1x_5}{W_1^2|x_5|}-\frac{F_0\beta_2x_5}{W_2^2|x_5|}\right]x_{10}$$

$$
\begin{aligned}
\dot{V}(\mathbf{x}) \quad = \quad & \left\{\frac{1}{2}[(x_1-p_1)\cos x_3+(x_2-p_2)\sin x_3]\left[1+\sum_{i=1}^{2}\frac{\beta_i}{W_i}\right]+u_1\right\}x_6 \\
& +\left\{\frac{1}{2}[(x_1-p_1)\cos x_3+(x_2-p_2)\sin x_3]\left[1+\sum_{i=1}^{2}\frac{\beta_i}{W_i}\right]+u_2\right\}x_7 \\
& \{[(x_1-p_1)(-l_G\sin x_3-l_1\sin(x_3+x_4)-l_2\sin(x_3+x_4+x_5)) \\
& +(x_2-p_2)(l_G\cos x_3+l_1\cos(x_3+x_4)+l_2\cos(x_3+x_4+x_5))]\left[1+\sum_{i=1}^{2}\frac{\beta_i}{W_i}\right]+u_3\}x_8 \\
& \{[(x_1-p_1)(-l_1\sin(x_3+x_4)-l_2\sin(x_3+x_4+x_5)) \\
& +(x_2-p_2)(l_1\cos(x_3+x_4)+l_2\cos(x_3+x_4+x_5))]\left[1+\sum_{i=1}^{2}\frac{\beta_i}{W_i}\right]+u_4\}x_9 \\
& \{[(x_1-p_1)(-l_2\sin(x_3+x_4+x_5))+(x_2-p_2)(l_2\cos(x_3+x_4+x_5))] \\
& \left[1+\sum_{i=1}^{2}\frac{\beta_i}{W_i}\right]+u_5-F_0\left(\frac{\beta_1}{W_1^2}-\frac{\beta_2}{W_2^2}\right)\frac{x_5}{|x_5|}\}x_{10} \\
= \quad & \{G_1(\mathbf{x})+u_1\}x_6+\{G_2(\mathbf{x})+u_2\}x_7+\{G_3(\mathbf{x})+u_3\}x_8 \\
& +\{G_4(\mathbf{x})+u_4\}x_9+\{G_5(\mathbf{x})+u_5\}x_{10} \\
= \quad & \{G_1+u_1\}x_6+\{G_2+u_2\}x_7+\{G_3+u_3\}x_8+\{G_4+u_4\}x_9+\{G_5+u_5\}x_{10}
\end{aligned}
$$

A.6 Derivatives of components in Subsection 6.5.1

The separate components of $\dot{V}(\mathbf{x})$ are :

$$\begin{aligned}
\dot{V}_1(\mathbf{x}) &= (x_1 - p_1)\dot{x_1} + (x_2 - p_2)\dot{x_2} + x_6\dot{x_6} + x_7\dot{x_7} + x_8\dot{x_8} + x_9\dot{x_9} \\
&= (x_1 - p_1)[x_6 \cos x_3 - l x_7 \sin x_3 - x_7 l_1 \sin(x_3 + x_4) \\
&\quad -x_8 l_1 \sin(x_3 + x_4) - x_7 l_2 \sin(x_3 + x_4 + x_5) - x_8 l_2 \sin(x_3 + x_4 + x_5) \\
&\quad -x_9 l_2 \sin(x_3 + x_4 + x_5)] \\
&\quad +(x_2 - p_2)[x_6 \sin x_3 + l x_7 \cos x_3 + x_7 l_1 \cos(x_3 + x_4) \\
&\quad +x_8 l_1 \cos(x_3 + x_4) + x_7 l_2 \cos(x_3 + x_4 + x_5) + x_8 l_2 \cos(x_3 + x_4 + x_5) \\
&\quad +x_9 l_2 \cos(x_3 + x_4 + x_5)] \\
&\quad +x_6 u_1 + x_7 u_2 + x_8 u_3 + x_9 u_4
\end{aligned}$$

$$\begin{aligned}
\dot{F}_1(\mathbf{x}) \sum_{i=1}^{2} \frac{\beta_i}{W_i} &= \{(x_1 - p_1)[x_6 \cos x_3 - l x_7 \sin x_3 \\
&\quad -x_7 l_1 \sin(x_3 + x_4) - x_8 l_1 \sin(x_3 + x_4) - x_7 l_2 \sin(x_3 + x_4 + x_5) \\
&\quad -x_8 l_2 \sin(x_3 + x_4 + x_5) - x_9 l_2 \sin(x_3 + x_4 + x_5)] \\
&\quad +(x_2 - p_2)[x_6 \sin x_3 + l x_7 \cos x_3 \\
&\quad +x_7 l_1 \cos(x_3 + x_4) + x_8 l_1 \cos(x_3 + x_4) + x_7 l_2 \cos(x_3 + x_4 + x_5) \\
&\quad +x_8 l_2 \cos(x_3 + x_4 + x_5) + x_9 l_2 \cos(x_3 + x_4 + x_5)]\} \\
&\quad \left(\sum_{i=1}^{2} \frac{\beta_i}{W_i} \right)
\end{aligned}$$

$$-F_1(\mathbf{x}) \sum_{i=1}^{2} \frac{\beta_i \dot{W}_i}{{W_i}^2} = -\left[\frac{F_1 \beta_1 x_5}{W_1^2 |x_5|} - \frac{F_1 \beta_2 x_5}{W_2^2 |x_5|} \right] x_9$$

$$\begin{aligned}
\dot{V}(\mathbf{x}) &= \{[(x_1-p_1)\cos x_3+(x_2-p_2)\sin x_3]\left[1+\sum_{i=1}^{2}\frac{\beta_i}{W_i}\right]+u_1\}x_6 \\
&\quad+\{[(x_1-p_1)(-l\sin x_3-l_1\sin(x_3+x_4)-l_2\sin(x_3+x_4+x_5)) \\
&\quad+(x_2-p_2)(l\cos x_3+l_1\cos(x_3+x_4)+l_2\cos(x_3+x_4+x_5))] \\
&\quad\left[1+\sum_{i=1}^{2}\frac{\beta_i}{W_i}\right]+u_2\}x_7 \\
&\quad+\{[(x_1-p_1)(-l_1\sin(x_3+x_4)-l_2\sin(x_3+x_4+x_5)) \\
&\quad+(x_2-p_2)(l_1\cos(x_3+x_4)+l_2\cos(x_3+x_4+x_5))]\left[1+\sum_{i=1}^{2}\frac{\beta_i}{W_i}\right]+u_3\}x_8 \\
&\quad+\{[(x_1-p_1)(-l_2\sin(x_3+x_4+x_5)+(x_2-p_2)l_2\cos(x_3+x_4+x_5))]\left[1+\sum_{i=1}^{2}\frac{\beta_i}{W_i}\right] \\
&\quad+u_4-F_1\left(\frac{\beta_1}{W_1^2}-\frac{\beta_2}{W_2^2}\right)\frac{x_5}{|x_5|}\}x_9 \\
&= \{G_1(\mathbf{x})+u_1\}x_6+\{G_2(\mathbf{x})+u_2\}x_7+\{G_3(\mathbf{x})+u_3\}x_8+\{G_4(\mathbf{x})+u_4\}x_9 \\
&= \{G_1+u_1\}x_6+\{G_2+u_2\}x_7+\{G_3+u_3\}x_8+\{G_4+u_4\}x_9
\end{aligned}$$